Bayesian inference on the number of recurrent events: A joint model of recurrence and survival

Willem van den Boom[1,2]**, Maria De Iorio**[2,3,4] **and Marta Tallarita**[4]

Abstract

The number of recurrent events before a terminating event is often of interest. For instance, death terminates an individual's process of rehospitalizations and the number of rehospitalizations is an important indicator of economic cost. We propose a model in which the number of recurrences before termination is a random variable of interest, enabling inference and prediction on it. Then, conditionally on this number, we specify a joint distribution for recurrence and survival. This novel conditional approach induces dependence between recurrence and survival, which is often present, for instance due to frailty that affects both. Additional dependence between recurrence and survival is introduced by the specification of a joint distribution on their respective frailty terms. Moreover, through the introduction of an autoregressive model, our approach is able to capture the temporal dependence in the recurrent events trajectory. A non-parametric random effects distribution for the frailty terms accommodates population heterogeneity and allows for data-driven clustering of the subjects. A tailored Gibbs sampler involving reversible jump and slice sampling steps implements posterior inference. We illustrate our model on colorectal cancer data, compare its performance with existing approaches and provide appropriate inference on the number of recurrent events.

*Prepared using *sagej.cls* [Version: 2017/01/17 v1.20]*

1 Introduction

Recurrent events arise in many applications including, amongst others, medicine, science and technology. Typical examples are given by recurrent infections, asthma attacks, hospitalizations, product repairs, and machine failures. Often, the number of recurrent events before termination of the process, such as by death or failure, is of interest. For instance, rehospitalizations are a major financial burden for the health system[1] and their number is used in policy making.[2,3] This work proposes a model which explicitly accounts for the number of recurrent events before termination by building on recent advances in joint modelling of recurrence and termination.

The two main statistical approaches to inference on recurrent events are (1) modelling the intensity or hazard function of the event counts process and (2) modelling the sequence of times between recurrent events, known as gap times or waiting times.[4] The first approach is most suitable when individuals frequently experience the recurrent event of interest and the occurrence does not alter the process itself. Here, we mention some examples that consider the dependence between recurrence and survival time. Liu et al.,[5] Rondeau et al.,[6] Ye et al.,[7] Huang et al.,[8] Sinha et al.[9] and Ouyang et al.[10] model the intensity of the recurrent events and the survival time. The latter two approaches propose Bayesian methods with an emphasis on modelling the risk of death and the risk of rejections for heart transplantation patients. Olesen and Parner,[11] Huang and Liu,[12] Yu and Liu,[13] Bao et al.[14] and Liu et al.[15] model the hazard function of the recurrent events and of the survival jointly, with the recurrent events and the survival being independent conditionally on frailty parameters. Yu et al.[16] model the intensity of the recurrent events and the hazard function of survival jointly while assuming independent censoring before death.

The second approach, which focuses on the sequence of gap times, is more appropriate when the recurrent events are relatively infrequent, when individual renewal takes place after an event, or when the goal is prediction of the time to the next event. Therefore, this approach is highly relevant for biomedical applications. For instance, major recurrent cardiac events for one patient are often rather infrequent from a statistical viewpoint. Also, healthcare planning can benefit from time-to-event predictions, especially

[1]Yale-NUS College, National University of Singapore, Singapore
[2]Singapore Institute for Clinical Sciences, Agency for Science, Technology and Research, Singapore
[3]Yong Loo Lin School of Medicine, National University of Singapore, Singapore
[4]Department of Statistical Science, University College London, UK

Corresponding author:
Willem van den Boom, Yale-NUS College, National University of Singapore, Singapore 138527, Singapore.
Email: willem@yale-nus.edu.sg

if events require hospitalization. Nonetheless, there is less existing work on the second approach than on the first. This work places itself within the second framework, as the events in our application are infrequent but measured on many individuals.

Using the second approach, Li et al.[17,18] define survival functions via a copula to allow for dependence between recurrence and survival conditionally on frailty parameters. Paulon et al.[19] and Tallarita et al.[20] propose Bayesian non-parametric models for the gap times, with the former also considering dependence with survival time. We take this previous work as a starting point with some important differences. Our autoregressive process for gap times has a constant mean, unlike Tallarita et al.,[20] as the process includes regression coefficients which would otherwise be hard to interpret. Unlike Paulon et al.,[19] we do not assume independence of gap times conditionally on random effects, and we have separate random effects for gap and survival times, enabling greater flexibility in capturing dependence or lack thereof between recurrence and survival.

The main novel methodological contribution of this work is to explicitly enable inference on the number of recurrent events preceding a termination event. Previous work[11,12,17–19] also considers termination of the observed recurrence process. In that work, a large number of recurrent events are assumed to exist for each individual with the recurrent event process defined also after the terminal event has occurred. Then, the gap times are censored either by the survival censoring time or by the actual survival time. The contribution to the likelihood of the gap times after censoring is set equal to one such that the assumed large number of censored gap times does not affect inference. It is preferable to avoid the often unrealistic assumption of a large arbitrary number of recurrent events or the continuation of the recurrence process beyond the terminal event. More importantly, these approaches prevent inference on the number of events before termination. This can constitute a major limitation in many applications. For example, there is a large literature[21–23] for hospitalizations on assessing the risk of recurrence for a time window such as within 30 days of hospital discharge as this has serious implications for healthcare cost. Our model can not only provide such risk estimates but is also able to infer the number of rehospitalizations which can aid healthcare planning (e.g. budgeting, provisioning).

We overcome the limitations of previous approaches by adopting a conditional approach. More in detail, we explicitly model the number of recurrent events before the terminal event. Then, conditionally on the number of events, we specify a joint distribution for gap times and survival. To the best of our knowledge, this modelling strategy has never been employed in the context of joint modelling of survival and recurrence processes. The resulting posterior inference is computationally more challenging than the models proposed in the available literature. We therefore develop a Markov chain Monte Carlo algorithm which relies on various computational tools such as reversible jump Markov chain Monte Carlo[24] and slice sampling.[25] Our explicit modelling of the number of recurrent events yields a more intuitive model specification, and captures the dependence structure between the recurrence and survival

processes, which is important in medical applications and beyond. The main motivating result though is intuitive inference and prediction for the number of recurrent events.

An important factor in medical applications related to recurrent events and survival time is the overall frailty. Increased frailty is often associated with both increased disease recurrence and reduced survival. Subject-specific random effects describe the frailty by informing both the survival time and the dependence of subsequent gap times. The random effects are modelled flexibly with a Dirichlet process DP,[26] prior as in Paulon et al.[19] and Tallarita et al.[20] It is well known that the DP is almost surely discrete. This feature is particularly useful in applications as it allows for data-driven clustering of observations. If G is DP(M, G_0) with concentration parameter M and base measure G_0, then it admits a stick-breaking representation[27] and can be represented as

$$G(\cdot) = \sum_{h=1}^{\infty} w_h \, \delta_{\boldsymbol{\theta}_h}(\cdot)$$

where $\delta_{\boldsymbol{\theta}_h}$ is a point mass at $\boldsymbol{\theta}_h$, the weights w_h follow the stick-breaking process $w_h = V_h \prod_{j<h}(1 - V_j)$ with $V_h \overset{\text{i.i.d.}}{\sim} \text{Beta}(1, M)$, and the atoms $\{\boldsymbol{\theta}_h\}_{h=1}^{\infty}$ are such that $\boldsymbol{\theta}_h \sim G_0$. The sequences $\{\boldsymbol{\theta}_h\}_{h=1}^{\infty}$ and $\{V_h\}_{h=1}^{\infty}$ are independent. The discreteness of G induces clustering of the subjects, based on the unique values of the random locations $\boldsymbol{\theta}_h$, where the number of clusters is learned from the data. This choice allows for extra flexibility, variability between individual trajectories, overdispersion and clustering of observations, and overcomes the often too restrictive assumptions underlying a parametric random effects distribution.

Paulon et al.[19] specify a single random effects parameter which influences both the distribution of the gap times and the distribution of survival. Instead, we introduce different random effects parameters, one for the recurrence process and one for the survival. We model these jointly using a DP prior, ensuring dependence between recurrence and survival. Additionally, we specify an autoregressive model for the gap times to capture the dependence between subsequent gap times as some persistence of recurrence across time is expected. Tallarita et al.[20] also use an autoregressive model, but on the random effects instead of the gap times themselves.

The paper is structured as follows. Section 2 introduces the model. Section 3 checks its performance on simulated data. Section 4 discusses an application to colorectal cancer data. Section 5 compares our approach with existing ones. Section 6 concludes the paper.

2 Model

2.1 Notation

We consider data on L individuals. Let T_{i0} denote the start time of the recurrent event process for individual i. We assume $T_{i0} = 0$ for $i = 1, \ldots, L$. Let S_i denote the survival time for individual i since the start of the corresponding event process. Each individual i experiences N_i recurrent events over the time interval $(0, S_i]$. Let T_{ij} denote the jth event time for individual i. Then, the last event time T_{iN_i} is less than or equal to S_i.

Some event processes are right censored due to end of study, as in the application of Section 4, or loss to follow-up. We assume completely independent censoring. This contrasts with the survival time S_i which our model allows to depend on the event process. Let c_i denote the minimum of the censoring time and the survival time S_i for individual i, who is thus observed over the interval $(0, c_i]$. Let $n_i \leq N_i$ denote the number of events that are observed over the interval $(0, c_i]$. Either S_i or the censoring time is observed. If S_i is observed, then $N_i = n_i$ and $0 < T_{i1} < \cdots < T_{iN_i} \leq S_i = c_i$. If S_i is not observed, then $N_i \geq n_i$ and $S_i > c_i$ are unknown and object of inference. In this case, $0 < T_{i1} < \cdots < T_{in_i} \leq c_i < T_{i(n_i+1)} < \cdots < T_{iN_i} \leq S_i$. We define the log gap times as

$$Y_{ij} = \log(T_{ij} - T_{i(j-1)}), \tag{1}$$

for $j = 1, \ldots, N_i$. The q-dimensional vector $\boldsymbol{x}_i$ contains individual-specific covariates.

2.2 Likelihood specification

Firstly, we assume that the number of gap times N_i follows a negative binomial distribution with shape parameter r and mean λ independently for $i = 1, \ldots, L$. Conditionally on N_i, we specify a joint model for the log gap times $\boldsymbol{Y}_i = (Y_{i1}, \ldots, Y_{iN_i})^T$ and the survival time S_i. We define the joint density $p(\boldsymbol{Y}_i, S_i \mid \text{—})$ where the joint space is constrained by $T_{iN_i} \leq S_i$. This induces dependence among N_i, $\boldsymbol{Y}_i$ and S_i in a principled manner. We build on existing literature [19,20] by assuming that the gap times and survival times follow truncated log-normal distributions where the pairs $(\boldsymbol{Y}_i, S_i)$ are mutually independent for $i = 1, \ldots, L$, conditionally on the random effects, number of recurrent events N_i and the other parameters in the model. Conditionally on N_i, the joint distribution for $(\boldsymbol{Y}_i, S_i)$ contains two components:

$$p(\boldsymbol{Y}_i, S_i \mid \text{—}) \propto f(\boldsymbol{Y}_i \mid \text{—}) \, f(S_i \mid \text{—}) \, \mathbb{1}(T_{iN_i} \leq S_i) \tag{2}$$

one defining the recurrence process and one for the survival, where $T_{iN_i} = \sum_{j=1}^{N_i} e^{Y_{ij}}$ per (1). The dependence between the two processes is defined through the constraint on the joint space and the specification of a joint random effect distribution on the process specific parameters.

The random effects parameter for the gap times is the two-dimensional vector $\boldsymbol{m}_i$ which characterizes an autoregressive model for $\boldsymbol{Y}_i$ that captures dependence between subsequent gap times:

$$
\begin{aligned}
f(\boldsymbol{Y}_i \mid \boldsymbol{\beta}, \boldsymbol{m}_i, N_i, \sigma^2, \boldsymbol{x}_i) = \mathcal{N}(Y_{i1} \mid \boldsymbol{x}_i^T \boldsymbol{\beta} + m_{i1}, \sigma^2) \\
\times \prod_{j=2}^{N_i} \mathcal{N}\{Y_{ij} \mid \boldsymbol{x}_i^T \boldsymbol{\beta} + m_{i1} + m_{i2}(Y_{i(j-1)} - \boldsymbol{x}_i^T \boldsymbol{\beta} - m_{i1}), \sigma^2\}, \quad (3)
\end{aligned}
$$

for $N_i \geq 1$. When $N_i = 0$, then we assume that $f(\boldsymbol{Y}_i \mid \boldsymbol{\beta}, \boldsymbol{m}_i, N_i, \sigma^2, \boldsymbol{x}_i)$ is equal to a constant. The q-dimensional vector $\boldsymbol{\beta}$ consists of covariate effects on the gap times. This resembles the autoregressive model on the random effects in Equation 2 of Tallarita et al.[20] Two main differences are due to the fact that the the mean of Y_{ij} is the same for all j conditionally on the remaining parameters in our model and that Tallarita et al.[20] do not consider a survival process, which implies the truncation $T_{iN_i} \leq S_i$ in our work. The truncation results from our conditioning on N_i whereas existing literature[19,20,28] specifies the likelihood as a joint distribution of the number of events n_i observed over the interval $(0, c_i]$ and their log gap times $Y_{i1}, \ldots, Y_{in_i}$. The regression coefficient $\boldsymbol{\beta}$ in (3) has the usual interpretation since the mean of Y_{ij} equals $\boldsymbol{x}_i^T \boldsymbol{\beta} + m_{i1}$ for all j.

The survival component of the model is proportional to a log-normal density:

$$
f(S_i \mid \boldsymbol{\gamma}, \delta_i, \boldsymbol{x}_i) = \mathcal{LN}\left\{S_i \mid \boldsymbol{x}_i^T \boldsymbol{\gamma} + \delta_i, \eta^2\right\} \tag{4}
$$

where the q-dimensional vector $\boldsymbol{\gamma}$ consists of covariate effects on the survival time and δ_i denotes a random effects parameter. Covariate effects can differ between gap and survival times, for instance if a therapy delays disease recurrence but does not prolong survival. Therefore, the model on the gap times in (3) and on the survival times in (4) have distinct regression coefficients $\boldsymbol{\beta}$ and $\boldsymbol{\gamma}$, respectively. Ultimately, due to the use of a DP prior on $(\boldsymbol{m}_i, \delta_i)$ our sampling model is an infinite mixture with weights and location deriving from the Dirichlet Process.[29,30] This allows us to overcome the often too restrictive assumptions imposed by a choice of a parametric model.

2.3 Prior specification

We specify a non-parametric prior for the random effects parameters $\boldsymbol{m}_i$ and δ_i in (3) and (4). In more detail, $(\boldsymbol{m}_i, \delta_i) \sim G$ independently for $i = 1, \ldots, L$, where $G \sim \text{DP}(M, G_0)$,

with $M \sim \text{Gamma}(a_M, b_M)$ and base measure $G_0 = \mathcal{N}_2(\mathbf{0}_{2\times1}, \sigma_m^2 \boldsymbol{I}_2) \times \mathcal{N}(0, \sigma_\delta^2)$. Finally, the prior distributions on the remaining parameters are $\boldsymbol{\beta} \sim \mathcal{N}_q(\mathbf{0}_{q\times1}, \sigma_\beta^2 \boldsymbol{I}_q)$, $\boldsymbol{\gamma} \sim \mathcal{N}_q(\mathbf{0}_{q\times1}, \sigma_\gamma^2 \boldsymbol{I}_q)$, $\sigma^2 \sim \text{Inv-Gamma}(\nu_{\sigma^2}/2, \nu_{\sigma^2} \sigma_0^2/2), \eta^2 \sim \text{Inv-Gamma}(\nu_{\eta^2}/2, \nu_{\eta^2} \eta_0^2/2), r \sim \text{Gamma}(a_r, b_r)$ and $\lambda \sim \text{Gamma}(a_\lambda, b_\lambda)$.

2.4   Posterior inference

Posterior inference is performed through a Gibbs sampler algorithm. This includes imputing N_i, $Y_{i(n_i+1)}, \ldots, Y_{iN_i}$ and S_i for each censored individual i by sampling them according to the model in Section 2.2. The Gibbs update for N_i and $\boldsymbol{Y}_i$ is transdimensional since the number of events N_i represents the dimensionality of the sequence of log gap times $\boldsymbol{Y}_i$. This requires devising a reversible jump sampler[24] for N_i and $\boldsymbol{Y}_i$.

Most full conditional distributions are intractable due to the truncation $T_{iN_i} \leq S_i$, which for instance causes the normalization constant of $p(\boldsymbol{Y}_i, S_i \mid \text{---})$ to depend on parameters of interest. We use slice sampling[25] to deal with this intractability. The normalization constant of $p(\boldsymbol{Y}_i, S_i \mid \text{---})$ is also intractable. We therefore approximate it using the Fenton-Wilkinson[31] method. Algorithm 8 from Neal[32] is implemented to sample the DP parameters $(\boldsymbol{m}_i, \delta_i)$. Section S1 of the supplemental material details and derives the Markov chain Monte Carlo algorithms.

3   Simulation study

We investigate the performance of our model and the Markov chain Monte Carlo algorithm via a simulation study. We consider $L = 150$ individuals spread across three clusters of size 50 each by assigning every first, second and third individual to Cluster 1, 2 and 3, respectively, and $q = 2$ covariates which are drawn independently from a standard uniform distribution. Then, we sample data according to the likelihood in Section 2.2 with $\boldsymbol{\beta} = \boldsymbol{\gamma} = (-1, 1)^T, r = 1, \lambda = 7, \sigma^2 = 1, \eta^2 = 1, \boldsymbol{m}_h^* = \{h, 0.8\,(h - 2)\}^T$ and $\delta_h^* = h + 4$ where $\boldsymbol{m}_h^* = \boldsymbol{m}_i$ and $\delta_h^* = \delta_i$ if and only if individual i belongs to the hth cluster for $h = 1, 2, 3$. From these simulated data, we construct four different scenarios, namely where 0%, 50%, 80% and 90% of the individuals, selected uniformly at random, are censored. The censoring times c_i are sampled uniformly from the time interval (T_{i1}, S_i) between the first event recurrence and death similarly to the simulation in Section 4 of Tallarita et al.[20] if $N_i \geq 1$, and from $(0, S_i)$ otherwise.

We choose hyperparameters yielding uninformative prior distributions as detailed in Section S2 of the supplemental material. The base measure G_0 of the DP prior has high variance. A priori, σ^2 and η^2 have an expected value of one and a variance of 100. We run the Gibbs sampler for 200 000 iterations, discarding the first 20 000 as burn-in and thinning every 10 iterations, resulting in a final posterior sample size of 18 000.

Figure 1. The number of gap times N_i (circle) and, if applicable, their posterior means (dot) and 95% posterior credible intervals (lines) for each individual from our model fitted on the simulated data. For censored individuals, the number of observed gap times n_i is marked by '$\times$'.
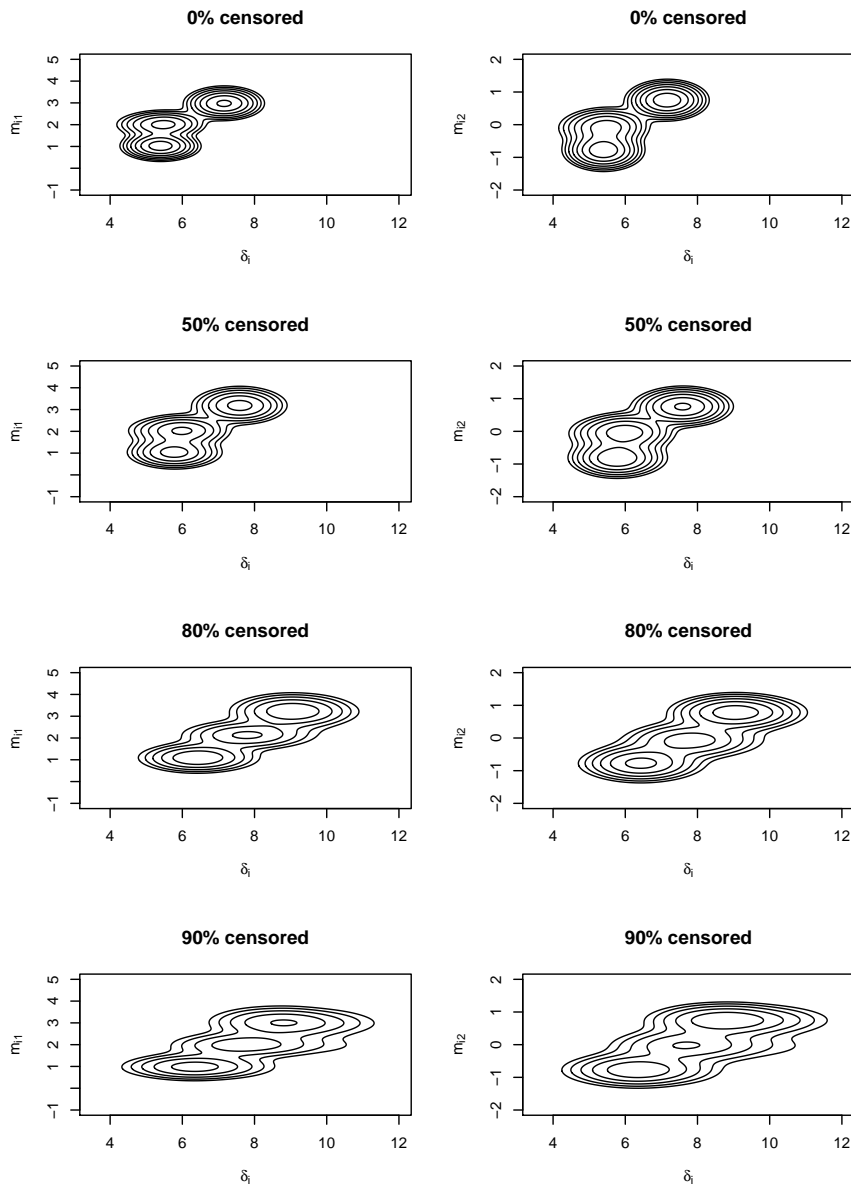
Figure 2. Contour plots of the log of the bivariate posterior predictive densities of (m_{i1}, δ_i) (left) and (m_{i2}, δ_i) (right) for a hypothetical new individual from the simulated data.
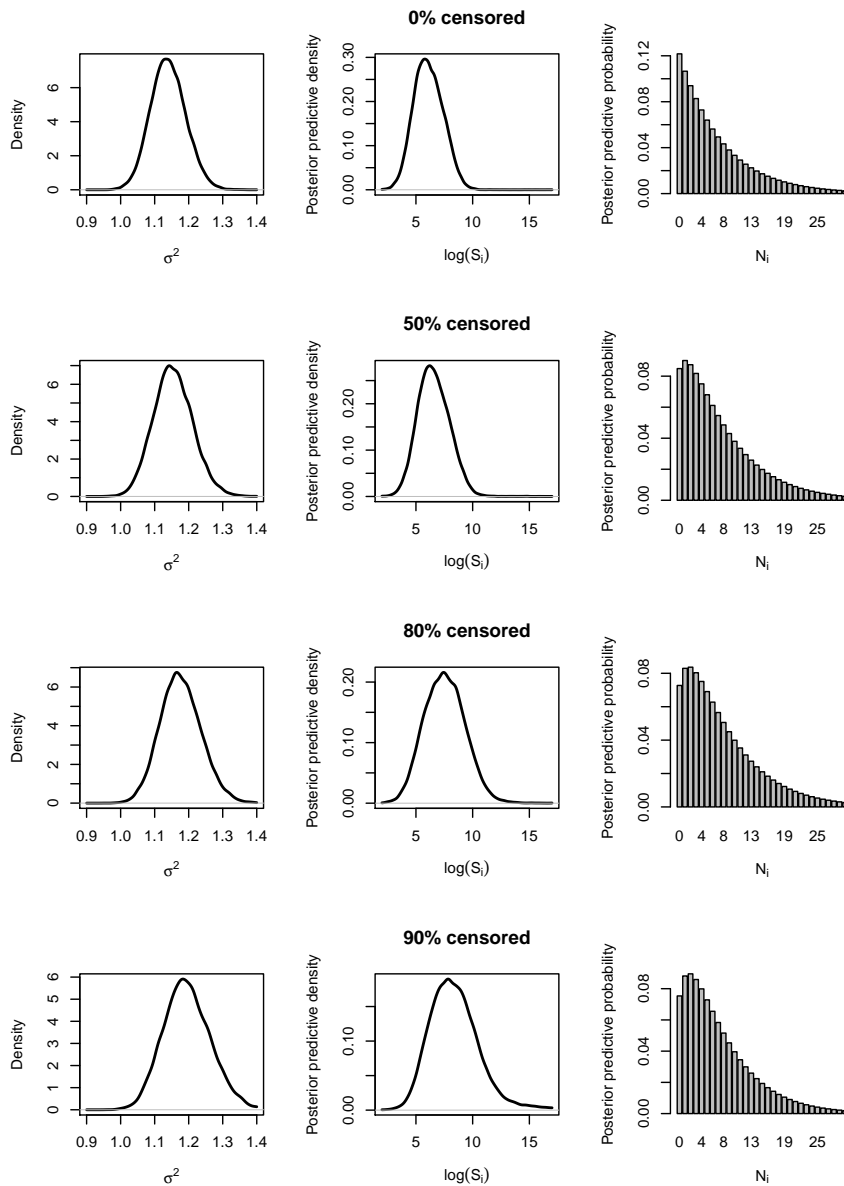
Figure 3. Posterior density for σ^2, and posterior predictive density for $\log(S_i)$ and posterior predictive probability mass function for N_i for a hypothetical new patient with covariates equal to their sample medians from our model fitted on the simulated data.
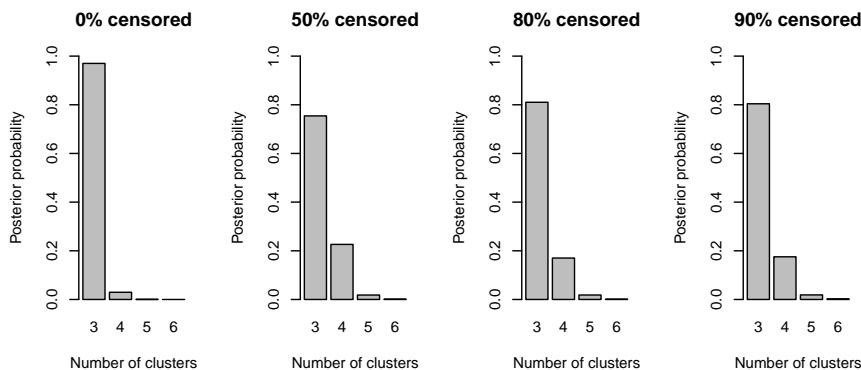
Figure 4. Posterior distribution of the number of clusters from our model fitted on the simulated data.
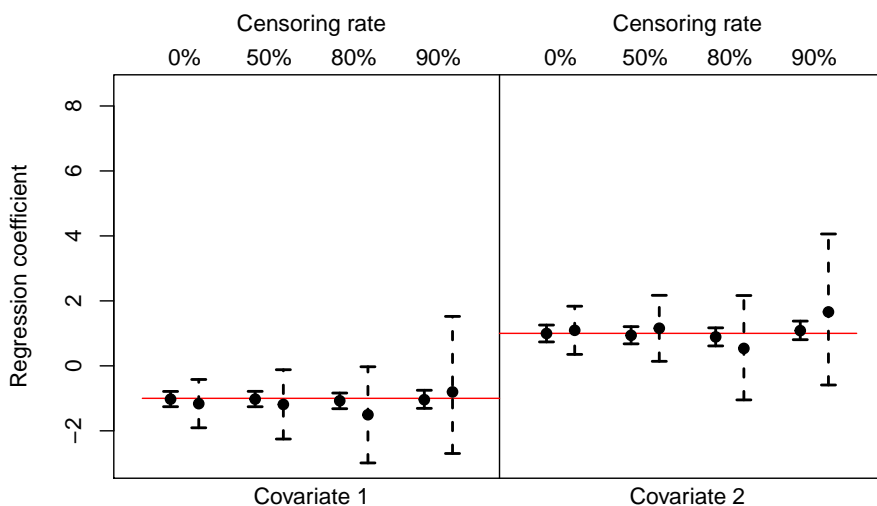

Figure 5. Posterior means (dot) and 95% marginal posterior credible intervals (lines) of the regression coefficients from our model fitted on the simulated data. The solid lines represent credible intervals for the regression coefficients β in (3) for the gap times model. The dashed lines correspond with the regression coefficients γ in (4) for the survival times. The horizontal line marks the true $\beta = \gamma = (-1, 1)^T$ from which the data were simulated.

Figures 1 through 5 summarize the results. The predictions and uncertainty quantification for the number of recurrent events N_i in Figure 1 are sensible with only 16 (5%) of the 330 credible intervals not covering the true N_i. Figures 2 and 3 show increased posterior uncertainty for higher levels of censoring.

Table 1. Frequency table of the number of observed gap times n_i and, for the 109 uncensored patients, the total number of gap times N_i in the colorectal cancer data.

n_i	0	1	2	3	4	5	6	7	8	9	10	11	16	22
Frequency (all)	199	105	45	21	15	8	4	0	1	1	1	1	1	1
Frequency (uncensored)	36	33	16	10	6	4	0	0	1	1	0	0	1	1

This increase in uncertainty is larger for δ_i, which relates to the survival time S_i, than for other parameters which relate to the recurrence process. A reason for this is that, for a censored individual i, often some event times are observed while S_i is right-censored and thus not observed. The posterior mass on the actual number of clusters is marginally higher for the uncensored than for the censored data in Figure 4, although it must be noticed that posterior inference on K is robust across different level of censoring. Figure 5 shows accurate inference for $\boldsymbol{\beta}$ with the uncertainty in $\boldsymbol{\gamma}$ increasing with the censoring rate as a higher censoring induces more uncertainty about the survival time S_i.

Section S3 of the supplemental material contains additional simulation studies. Our simulations show that poster inference is robust not only to the choice of hyper-parameters of the negative binomial distribution, but also to model misspecification. Nevertheless, it must be noted that posterior mean estimates and their associated bias and mean squared errors are affected by censoring rate.

4 Application to colorectal cancer data

4.1 Data description and analysis

We apply our model to the colorectal cancer data described in Gonzalez et al.[33] which consider $L = 403$ patients diagnosed with colorectal cancer between 1996 and 1998 in Bellvitge University Hospital in Barcelona, Spain. The data consist of hospital readmissions related to colorectal cancer surgery up until 2002 and are available as part of the R package `frailtypack`.[34] The date of surgery represents the origin of a patient's recurrence process such that $T_{i0} = 0$ for all i. Consequently, n_i represents the number of observed gap times between subsequent hospitalizations. Patients experience between zero and 22 hospitalizations each and $\sum_{i=1}^{L} n_i = 458$ in aggregate. Table 1 shows how they are distributed across patients. Gap times are defined as the difference between successive hospitalizations and, as such, capture both the length of stay in the hospital and the time between discharge and the next hospitalization.

The main clinical outcome of interest is deterioration to death. We therefore define the survival time S_i as the time to death. The survival times of 294 out of the 403 recurrence processes are censored due to the follow-up ending in 2022, resulting in unobserved total number of gap times N_i.

Patient characteristics considered are the binary variables 1) whether the patient received radiotherapy or chemotherapy and 2) gender, and Dukes' tumour classification which takes as levels stage A-B, C
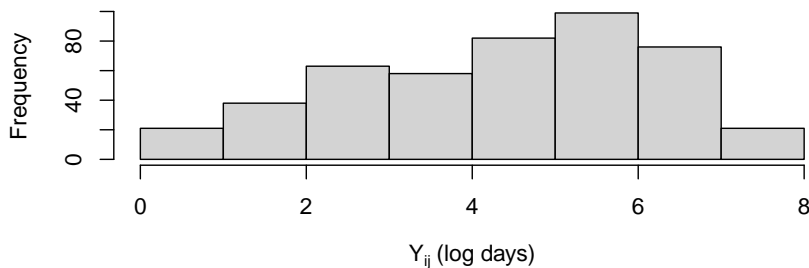
Figure 6. Histogram of the 458 observed log gap times Y_{ij} in the colorectal cancer data.
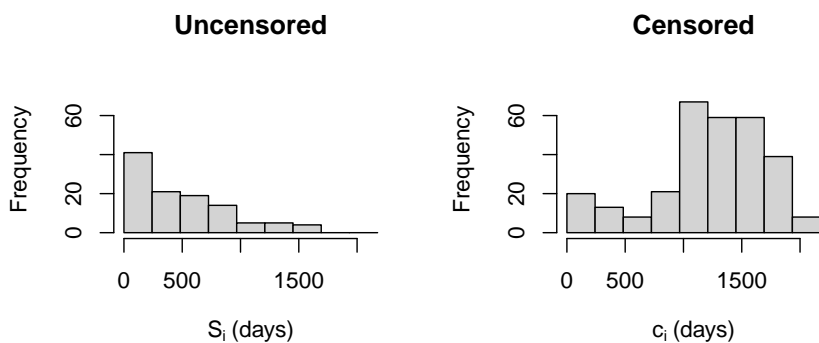

Figure 7. Histograms of the log of the 109 observed survival times S_i (left) and the 294 censoring times (right) in the colorectal cancer data. If the survival time S_i is observed, then $c_i = S_i$.

or D. We dummy code Dukes' classification with stage A-B as baseline resulting in a subject-specific 4-dimensional covariate vector $\boldsymbol{x}_i$, with $q = 4$. Table 2, and Figures 6 and 7 summarize the patient characteristics, and the gap and survival times.

We use the same priors, from Section S2 of the supplemental material, and set-up of the Gibbs sampler as the simulation study in Section 3. Then, the regression coefficients $\boldsymbol{\beta}$ and $\boldsymbol{\gamma}$ have high prior variance.
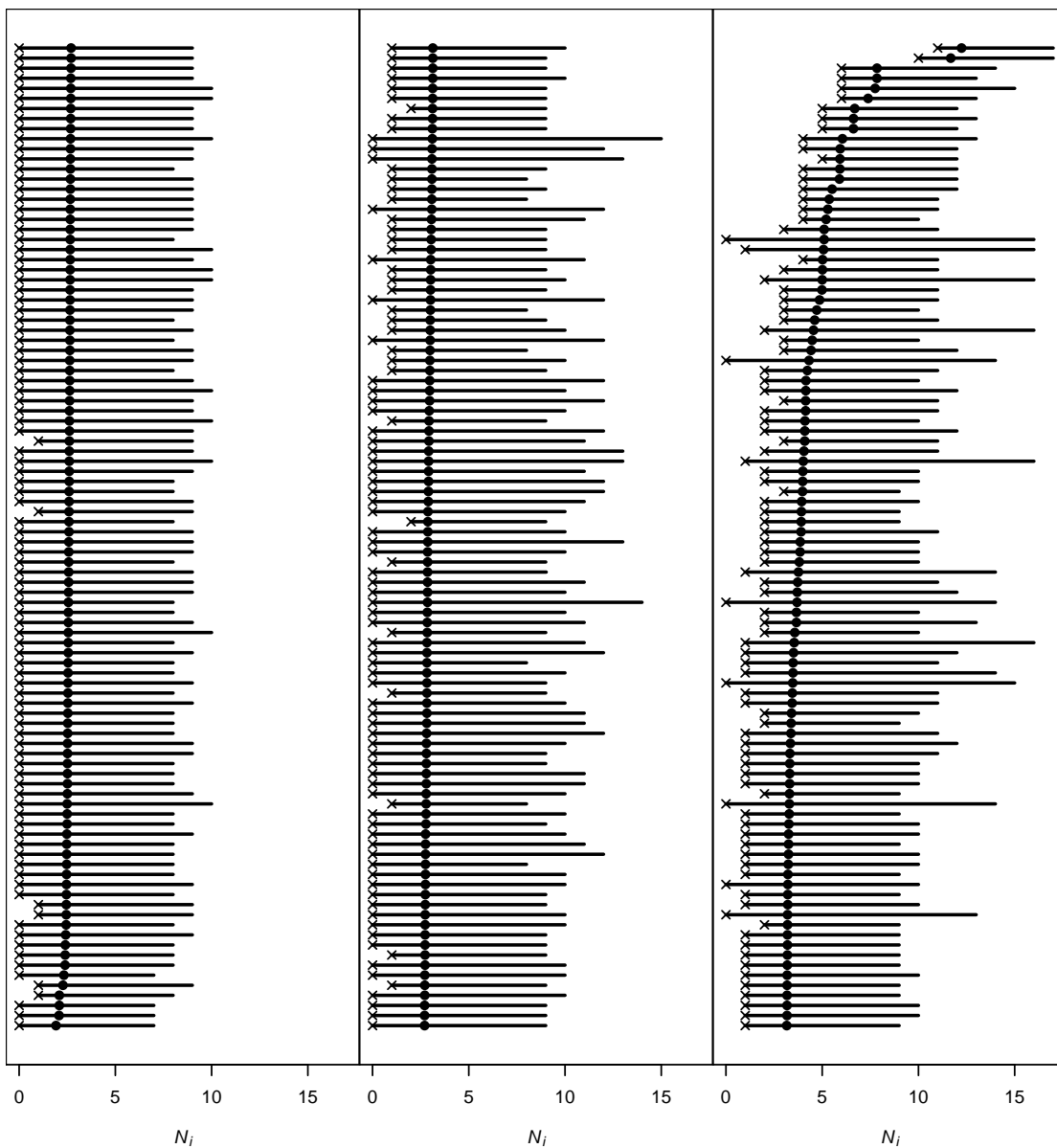
Figure 8. The posterior means (dot) of the number of gap times N_i and 95% posterior credible intervals (lines) for each censored patient from our model fitted on the colorectal cancer data. The number of observed gap times n_i is marked by '$\times$'.
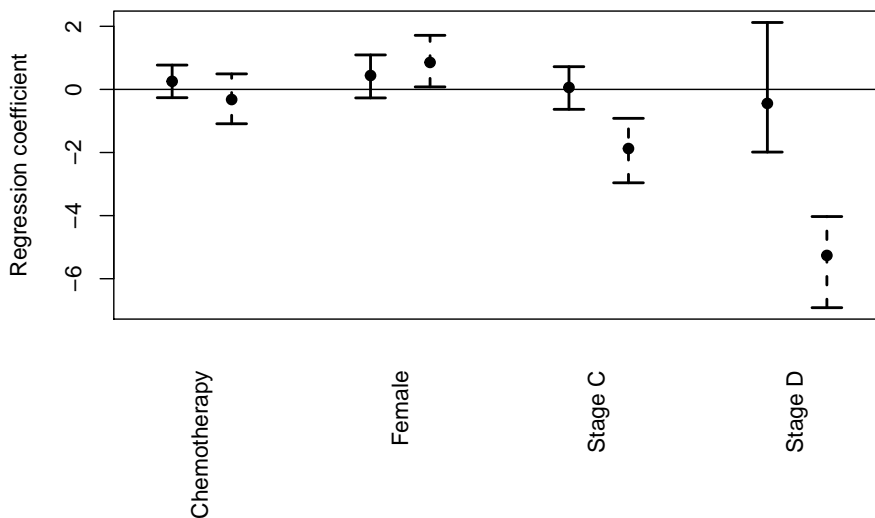
Figure 9. Posterior means (dot) and 95% marginal posterior credible intervals (lines) of the regression coefficients from our model fitted on the colorectal cancer data. The solid lines represent credible intervals for the regression coefficients β in (3) for the gap times model. The dashed lines correspond with the regression coefficients γ in (4) for the survival times.

4.2 Posterior inference on the number of recurrent events

Figure 8 summarizes the posterior distribution of the total number of gap times N_i for each censored patient. The posterior means for the censored N_i are generally in line with the observed N_i in Table 1 though the lowest posterior mean is with 1.9 higher than the lowest observed N_i. This is expected since patients with longer survival times S_i are both more likely to have a higher number of gap times N_i and to be censored due to end of study. Our model flexibly captures N_i's uncertainty, which varies notably across censored patients. These findings highlight the importance of modelling and inferring N_i when the number of events is censored and, therefore, unknown.

4.3 Posterior inference on the regression coefficients

The regression coefficients β and γ capture the covariate effects on the recurrent event and survival processes, respectively. Figure 9 shows negative coefficients for the more advanced tumour stages C and D in the survival regression but not for the gap times model. This suggests that more severe tumours, while they negatively affect survival, do not have an effect on rehospitalization rate beyond the link between survival and hospitalization implied by our joint model.
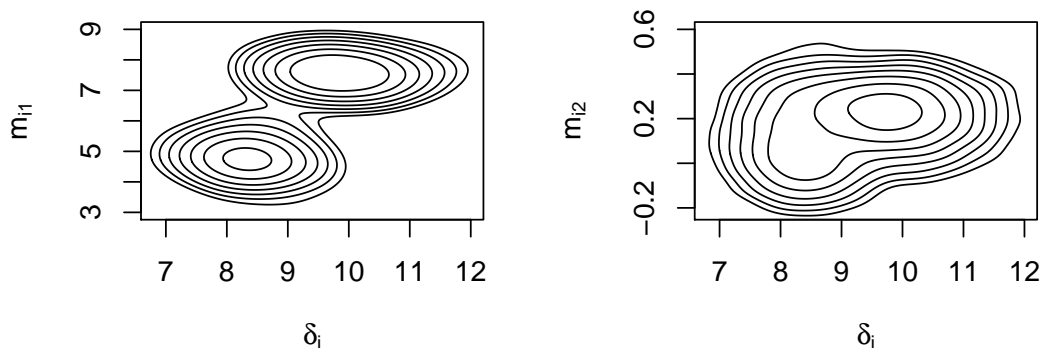
Figure 10. Contour plots of the log of the bivariate posterior predictive densities of (m_{i1}, δ_i) (left) and (m_{i2}, δ_i) (right) for a hypothetical new patient from the colorectal cancer data.

4.4 Posterior inference on the cluster allocation

As discussed in Section 1, the DP prior on $(\boldsymbol{m}_i, \delta_i)$ described in Section 2.3 allows for clustering of patients based on their recurrent event and survival profiles. The random effects parameters determine the clustering of patients and capture the dependence between the recurrence and survival processes. Indeed, the posterior predictive distribution of these parameters for a hypothetical new patient is multimodal as shown in Figure 10, indicating the presence of multiple patient subpopulations. The clustering depends on both gap time trajectories and survival outcomes thanks to the joint distribution on $\boldsymbol{m}_i$ and δ_i. In particular, Figure 10 reports the bivariate posterior marginals of (m_{i1}, δ_i) and (m_{i2}, δ_i), which are bimodal.

Posterior inference on the clustering structure of the patients is of clinical interest as it might guide more targeted therapies. Our Gibbs sampler provides posterior samples of the cluster allocation. Here, we report the cluster allocation that minimizes the posterior expectation of Binder's[35] loss function under equal misclassification costs, which is a common choice in the applied Bayesian non-parametrics literature.[36] See Appendix B of Argiento et al.[37] for computational details. Briefly, Binder's loss function measures the difference for all possible pairs of individuals between the true probability of co-clustering and the estimated cluster allocation. In this context, the posterior estimate of the partition of the patients has three clusters, with 99% of the patients allocated to two clusters which are summarized in Table 2. The largest cluster, Cluster 1, has longer gap and imputed survival times than Cluster 2. Moreover, the

Table 2. Summary statistics of the colorectal cancer data and the posterior from our model. The two clusters are the largest from a posterior estimate of the cluster allocation that minimizes the posterior expectation of Binder's [35] loss function. The averages and standard deviations of posterior means are taken across patients and recurrent events. S_i is recorded in days and Y_{ij} in log days.

|	Full dataset	Cluster 1	Cluster 2
Number of patients	403	292	108
Proportion censored	73%	81%	54%
Average uncensored N_i	1.78 (2.92)	0.79 (0.93)	2.68 (3.41)
Average posterior mean of N_i (SD)	2.87 (1.95)	2.55 (1.08)	3.66 (2.91)
Average uncensored Y_{ij} (SD)	4.35 (1.84)	5.55 (1.24)	3.91 (1.72)
Average posterior mean of Y_{ij} (SD)	6.55 (1.39)	7.06 (0.82)	5.03 (1.52)
Average uncensored $\log(S_i)$ (SD)	5.78 (1.03)	5.66 (1.09)	5.96 (0.93)
Average posterior mean of $\log(S_i)$ (SD)	8.91 (2.14)	9.39 (2.03)	7.72 (1.85)
Proportion on chemotherapy	54%	55%	50%
Proportion female	41%	42%	37%
Proportion stage C	37%	34%	45%
Proportion stage D	19%	19%	17%
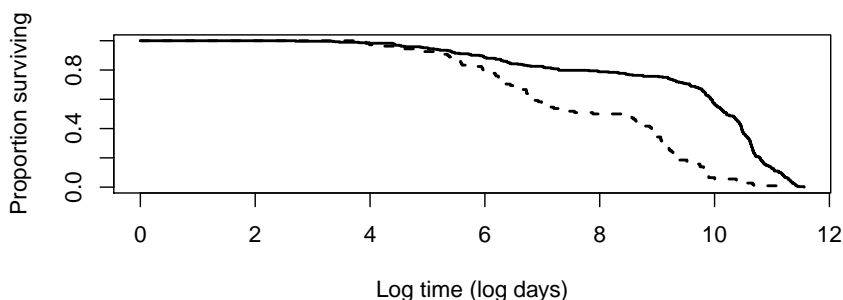
Figure 11. Kaplan-Meier survival estimates for the two largest clusters estimated by minimizing the expectation of Binder's [35] loss function under the posterior from our model on the colorectal cancer data. The solid and dashed lines represent Cluster 1 and 2, respectively. The curves are based on the posterior means of $\log(S_i)$.

Kaplan-Meier curves of each cluster in Figure 11 support the conclusion that Cluster 1 includes patients with longer survival times than Cluster 2. As shown in Table 2, Cluster 1 has a higher censoring rate than Cluster 2, as one might expect at longer survival times. The lower prevalence of late stage tumours in Cluster 1 also confirms that it includes healthier subjects than Cluster 2.

Figures S17 and S18 in the supplemental material contain additional posterior results. Section S4 of the supplemental material presents an application to atrial fibrillation data.

5   Comparison with other models

5.1   Cox proportional hazards model

We now compare our results on the colorectal cancer data to those obtained from the Cox proportional hazards model which is one of the most popular semi-parametric models in survival analysis with covariates. In this model, the hazard function for mortality is $h_i(t \mid \boldsymbol{\theta}) = h_0(t) \exp(\boldsymbol{z}_i^T \boldsymbol{\theta})$ where $h_0(t)$ is the baseline hazard function, $\boldsymbol{z}_i$ is a vector of covariates and $\boldsymbol{\theta}$ is a vector of regression coefficients. Here, a larger value of $\boldsymbol{z}_i^T \boldsymbol{\theta}$ leads to shorter survival times. This contrasts with (4) from our model where a larger $\boldsymbol{x}_i^T \boldsymbol{\gamma}$ is associated with longer survival times.

Our model allows for dependence between the gap and survival times. Therefore, for a fairer comparison when fitting the Cox proportional hazard model, we include a patient's log mean gap time in the covariate vector $\boldsymbol{z}_i$ in addition to the four covariates included in $\boldsymbol{x}_i$ described in Section 4.1. As a result, the 199 individuals with no observed gap times are excluded. Table S6 in the supplemental material shows the covariate effects on survival from the Cox proportional hazards model. The statistically significant effects agree with those from our model in Figure 9.

5.2   Joint frailty model

We also compare our model with the joint frailty model by Rondeau et al.[6] as implemented in the R package `frailtypack`.[34] The model estimates the hazard functions of rehospitalization and mortality jointly using two patient-specific frailty terms, namely u_i and v_i. The frailty term u_i captures the association between rehospitalization and mortality while v_i appears solely in the rehospitalization rate. Specifically, the hazard functions are $r_i(t \mid u_i, v_i, \boldsymbol{\beta}) = u_i \, v_i \, r_0(t) \, \exp(\boldsymbol{x}_i^T \boldsymbol{\beta})$ for rehospitalization and $\lambda_i(t \mid u_i, \boldsymbol{\gamma}) = u_i \, \lambda_0(t) \, \exp(\boldsymbol{x}_i^T \boldsymbol{\gamma})$ for mortality. Here, $r_0(t)$ and $\lambda_0(t)$ are baseline hazard functions, and $\boldsymbol{x}_i$, $\boldsymbol{\beta}$ and $\boldsymbol{\gamma}$ are defined as in Section 2. The random effects distributions are specified as follows: $v_i \sim \text{Gamma}(1/\rho, \, 1/\rho)$ and $u_i \sim \text{Gamma}(1/\epsilon, \, 1/\epsilon)$ independently for $i = 1, \ldots, L$.

The comparison of the joint frailty model results in Table S7 of the supplemental material with our results in Figure 9 shows that both models find that late stage tumours are associated with shorter survival. For the other covariates, the comparison is inconclusive with the joint frailty model finding statistically significant effects where our model does not and vice versa.

Finally, the estimate of ρ is 0.007 with a standard error of 0.001. This suggests heterogeneity between patients that is not explained by the covariates. The estimate of ϵ is 0.073 with a standard error of 0.13.

This implies that the rate of rehospitalizations is positively associated with mortality. These results are in line with the posterior clustering results from our model in Table 2 where Cluster 1 is characterized by both the longest gap times and the longest survival times.

5.3 Bayesian semi-parametric model from Paulon et al.[19]

For a more direct comparison, we consider the method proposed by Paulon et al.[19] as it models the gap and survival times jointly using Bayesian non-parametric priors. Paulon et al.[19] assume that, conditionally on all parameters and random effects, the gap times are independent of both each other and the survival time. This contrasts with the temporal dependence between gap times in (3). Shared random effects induce dependence between different gap times of the same patient. Specifically, Paulon et al.[19] assume $Y_{ij} \sim \mathcal{N}(\boldsymbol{x}_i^T \boldsymbol{\beta} + \alpha_i,\, \sigma_i^2)$ independently for $j = 1, \ldots, n_i + 1$ and $i = 1, \ldots, L$, and

$$\log(S_i) \sim \mathcal{N}(\boldsymbol{x}_i^T \boldsymbol{\gamma} + \psi\, \alpha_i,\, \eta^2), \tag{5}$$

independently for $i = 1, \ldots, L$, where $\boldsymbol{x}_i$, $\boldsymbol{\beta}$ and $\boldsymbol{\gamma}$ are defined as in Section 2, and α_i and σ_i are random effects. Paulon et al.[19] do not model the total number of gap times N_i but assume that each patient has a censored $(n_i + 1)$th log gap time $Y_{i(n_i+1)}$. They also assume a priori independence among $\boldsymbol{\beta}$, $\boldsymbol{\gamma}$, ψ, η and $(\boldsymbol{\alpha}, \boldsymbol{\sigma}^2)$. The random effects $(\alpha_i, \sigma_i^2) \sim G$ independently for $i = 1 \ldots, L$ where $G \sim \mathrm{DP}(M, G_0)$ with $M \sim \mathrm{Uniform}(a_M, b_M)$ and $G_0 = \mathcal{N}(0, \alpha_0^2) \times \mathrm{Inv\text{-}Gamma}(a_\sigma, b_\sigma)$. The priors on $\boldsymbol{\beta}$, $\boldsymbol{\gamma}$ and η^2 are set as in Section 2.3. Finally, $\psi \sim \mathcal{N}(0, \psi_0^2)$.

In fitting this model to the colorectal cancer data, we specify the same $\boldsymbol{x}_i$ and the same hyperparameters for the priors on $\boldsymbol{\beta}$, $\boldsymbol{\gamma}$ and η^2 as in Section 4.1. Furthermore, we set $a_M = 0.3$, $b_M = 5$, $\alpha_0^2 = 100$, $a_\sigma = 2.01$, $b_\sigma = 1.01$ and $\psi_0^2 = 100$. This model yields conclusions that are largely consistent with those from our model. In particular, the posterior distributions on the coefficients in Figure S19 of the supplemental material mimic our results in Figure 9 except for the effect of tumour stage on recurrence. Also, the posterior on ψ in (5) concentrates between 1.3 and 1.7 per Figure S20 of the supplemental material. This parameter captures the strength of the relationship between gap and survival times. Thus, the time between hospitalizations and survival have a positive association. This is consistent with the clustering results obtained from our model in Table 2. Lastly, the posterior on the number of clusters for this model and our model vary slightly, with a mode of three clusters for our model in Figure S18 of the supplemental material while Figure S21 of the supplemental material has the mode at five for the model from Paulon et al.[19] This is not surprising as our model introduces more structure: a temporal model for the gap time, as well as process-specific frailty terms which are jointly modelled non-parametrically. Moreover, the number of recurrent events is a random quantity and object of inference, which also informs the dependence between the two processes, in addition to the truncation $T_{iN_i} \leq S_i$ of (3).

In contrast, Paulon et al.[19] can capture such dependence using only ψ in (5), and the gap times are conditionally independent given ψ and the remaining parameters, with the total number of gap times per individual assumed arbitrarily large.

6 Discussion

We introduce a joint model on recurrence and survival that explicitly treats the number of recurrent events N_i before the terminal event as a random variable and object of inference as N_i is often of interest in applications. Additionally, the explicit modelling of N_i as well as the specification of a joint distribution for the random effects of the recurrence and survival processes induces dependence between these processes. Moreover, temporal dependence among recurrent events is introduced through a first-order autoregressive process on the gap times. Extension to a more complex temporal structure is in principle straightforward. The model allows for estimating covariates effects on the recurrence and survival processes by introducing appropriate regression terms. Our model can readily accommodate a different prior on the number of recurrent events than the negative binomial distribution. For instance, an earlier version of this work[38] used a Poisson distribution. The use of a non-parametric prior as random effects distribution allows for extra flexibility, patient heterogeneity and data-driven clustering of the patients.

We use log-normal kernels for the non-parametric survival and gap time distributions. Use of different kernels is computationally impracticable as then the evaluation of the normalization constant of $p(\boldsymbol{Y}_i, S_i \mid —)$ becomes considerably more expensive. This evaluation is already the computational bottleneck of our method as it happens frequently as part of slice sampling at each iteration of the Gibbs sampler. The reasons why using different kernels is problematic are twofold: Firstly, the log-normal kernel for the gap times enables the Fenton-Wilkinson[31] approximation for the distribution of T_{iN_i}. Other kernels for the gap times might not enable such computationally efficient evaluations. For instance, Proposition 1 of El Bouanani and Ben-Azza[39] gives rise to an approximation when using a Weibull kernel which is computationally more involved than the Fenton-Wilkinson method. Secondly, the current combination of the Fenton-Wilkinson method and a log-normal survival kernel reduce the normalization constant of $p(\boldsymbol{Y}_i, S_i \mid —)$ to a tail probability of a univariate Gaussian as detailed in Section S1.1 of the supplemental material. A different survival kernel, say a Weibull kernel, would require computation which is an order of magnitude more expensive, such as numerical integration to evaluate the normalization constant, or further approximation.

The simulation study shows the effectiveness of posterior inference on the number of recurrent events N_i. Comparison with the Cox proportional hazards model, the joint frailty model[6] and the Bayesian semi-parametric model from Paulon et al.[19] yields consistent results, with few exceptions in the estimation of

covariate effects. This discrepancy might be the result of the fact that these models have fewer parameters and assume a single patient population while our model detects multiple subpopulations. Moreover, in our model specification a further level of dependence is introduced through the distribution of the number of gap times. More flexibility, if required by the application, could be achieved by including also the hyper-parameters of the distribution of the number of gap-times in the nonparametric component of the model.

Funding

Declaration of conflicting interests

The Authors declare that there is no conflict of interest.

Supplemental material

The supplemental material referenced in the text is available online. The code that generated the results in this paper is available at <https://github.com/willemvandenboom/condi-recur>.

References

1. Jencks SF, Williams MV and Coleman EA. Rehospitalizations among patients in the medicare fee-for-service program. *New England Journal of Medicine* 2009; 360(14): 1418–1428. DOI:10.1056/nejmsa0803563.

2. McIlvennan CK, Eapen ZJ and Allen LA. Hospital readmissions reduction program. *Circulation* 2015; 131(20): 1796–1803. DOI:10.1161/circulationaha.114.010270.

3. Zuckerman RB, Sheingold SH, Orav EJ et al. Readmissions, observation, and the hospital readmissions reduction program. *New England Journal of Medicine* 2016; 374(16): 1543–1551. DOI:10.1056/nejmsa1513024.

4. Cook RJ and Lawless JF. *The statistical analysis of recurrent events*. Springer, New York, 2007. DOI:10.1007/978-0-387-69810-6.

5. Liu L, Wolfe RA and Huang X. Shared frailty models for recurrent events and a terminal event. *Biometrics* 2004; 60(3): 747–756. DOI:10.1111/j.0006-341x.2004.00225.x.

6. Rondeau V, Mathoulin-Pelissier S, Jacqmin-Gadda H et al. Joint frailty models for recurring events and death using maximum penalized likelihood estimation: Application on cancer events. *Biostatistics* 2007; 8(4): 708–721. DOI:10.1093/biostatistics/kxl043.

7. Ye Y, Kalbfleisch JD and Schaubel DE. Semiparametric analysis of correlated recurrent and terminal events. *Biometrics* 2007; 63(1): 78–87. DOI:10.1111/j.1541-0420.2006.00677.x.

8. Huang CY, Qin J and Wang MC. Semiparametric analysis for recurrent event data with time-dependent covariates and informative censoring. *Biometrics* 2010; 66(1): 39–49. DOI:10.1111/j.1541-0420.2009.01266.x.

9. Sinha D, Maiti T, Ibrahim JG et al. Current methods for recurrent events data with dependent termination. *Journal of the American Statistical Association* 2008; 103(482): 866–878. DOI:10.1198/016214508000000201.

10. Ouyang B, Sinha D, Slate EH et al. Bayesian analysis of recurrent event with dependent termination: An application to a heart transplant study. *Statistics in Medicine* 2013; 32(15): 2629–2642. DOI:10.1002/sim.5717.

11. Olesen AV and Parner ET. Correcting for selection using frailty models. *Statistics in Medicine* 2006; 25(10): 1672–1684. DOI:10.1002/sim.2298.

12. Huang X and Liu L. A joint frailty model for survival and gap times between recurrent events. *Biometrics* 2007; 63(2): 389–397. DOI:10.1111/j.1541-0420.2006.00719.x.

13. Yu Z and Liu L. A joint model of recurrent events and a terminal event with a nonparametric covariate function. *Statistics in Medicine* 2011; 30(22): 2683–2695. DOI:10.1002/sim.4297.

14. Bao Y, Dai H, Wang T et al. A joint modelling approach for clustered recurrent events and death events. *Journal of Applied Statistics* 2012; 40(1): 123–140. DOI:10.1080/02664763.2012.735225.

15. Liu L, Huang X, Yaroshinsky A et al. Joint frailty models for zero-inflated recurrent events in the presence of a terminal event. *Biometrics* 2015; 72(1): 204–214. DOI:10.1111/biom.12376.

16. Yu Z, Liu L, Bravata DM et al. Joint model of recurrent events and a terminal event with time-varying coefficients. *Biometrical Journal* 2013; 56(2): 183–197. DOI:10.1002/bimj.201200160.

17. Li Z, Chinchilli VM and Wang M. A Bayesian joint model of recurrent events and a terminal event. *Biometrical Journal* 2019; 61(1): 187–202. DOI:10.1002/bimj.201700326.

18. Li Z, Chinchilli VM and Wang M. A time-varying Bayesian joint hierarchical copula model for analysing recurrent events and a terminal event: an application to the cardiovascular health study. *Journal of the Royal Statistical Society: Series C (Applied Statistics)* 2019; 69(1): 151–166. DOI:10.1111/rssc.12382.

19. Paulon G, De Iorio M, Guglielmi A et al. Joint modeling of recurrent events and survival: A Bayesian non-parametric approach. *Biostatistics* 2018; DOI:10.1093/biostatistics/kxy026. Kxy026.

20. Tallarita M, De Iorio M, Guglielmi A et al. Bayesian autoregressive frailty models for inference in recurrent events. *The International Journal of Biostatistics* 2020; 16(1): 1–18. DOI:10.1515/ijb-2018-0088.

21. Kansagara D, Englander H, Salanitro A et al. Risk prediction models for hospital readmission: A systematic review. *JAMA* 2011; 306(15): 1688. DOI:10.1001/jama.2011.1515.

22. Futoma J, Morris J and Lucas J. A comparison of models for predicting early hospital readmissions. *Journal of Biomedical Informatics* 2015; 56: 229–238. DOI:10.1016/j.jbi.2015.05.016.

23. Mahmoudi E, Kamdar N, Kim N et al. Use of electronic medical records in development and validation of risk prediction models of hospital readmission: systematic review. *BMJ* 2020; 369: m958. DOI:10.1136/bmj.m958.

24. Green PJ. Reversible jump Markov chain Monte Carlo computation and Bayesian model determination. *Biometrika* 1995; 82(4): 711–732. DOI:10.1093/biomet/82.4.711.

25. Neal RM. Slice sampling. *The Annals of Statistics* 2003; 31(3): 705–767. DOI:10.1214/aos/1056562461.

26. Ferguson TS. A Bayesian analysis of some nonparametric problems. *The Annals of Statistics* 1973; 1(2): 209–230.

27. Sethuraman J. A constructive definition of Dirichlet priors. *Statistica Sinica* 1994; 4(2): 639–650.

28. Aalen OO and Husebye E. Statistical analysis of repeated events forming renewal processes. *Statistics in Medicine* 1991; 10(8): 1227–1240. DOI:10.1002/sim.4780100806.

29. Lo AY. On a class of Bayesian nonparametric estimates: I. density estimates. *The Annals of Statistics* 1984; 12(1). DOI:10.1214/aos/1176346412.

30. De Iorio M, Johnson WO, Müller P et al. Bayesian nonparametric nonproportional hazards survival modeling. *Biometrics* 2009; 65(3): 762–771. DOI:10.1111/j.1541-0420.2008.01166.x.

31. Fenton L. The sum of log-normal probability distributions in scatter transmission systems. *IEEE Transactions on Communications* 1960; 8(1): 57–67. DOI:10.1109/tcom.1960.1097606.

32. Neal RM. Markov chain sampling methods for Dirichlet process mixture models. *Journal of Computational and Graphical Statistics* 2000; 9(2): 249–265. DOI:10.1080/10618600.2000.10474879.

33. González JR, Fernandez E, Moreno V et al. Sex differences in hospital readmission among colorectal cancer patients. *Journal of Epidemiology & Community Health* 2005; 59(6): 506–511. DOI:10.1136/jech.2004.028902.

34. Rondeau V, Mazroui Y and Gonzalez JR. frailtypack: An R package for the analysis of correlated survival data with frailty models using penalized likelihood estimation or parametrical estimation. *Journal of Statistical Software* 2012; 47(4): 1–28. DOI:10.18637/jss.v047.i04.

35. Binder DA. Bayesian cluster analysis. *Biometrika* 1978; 65(1): 31–38.

36. Lau JW and Green PJ. Bayesian model-based clustering procedures. *Journal of Computational and Graphical Statistics* 2007; 16(3): 526–558.

37. Argiento R, Cremaschi A and Guglielmi A. A "density-based" algorithm for cluster analysis using species sampling Gaussian mixture models. *Journal of Computational and Graphical Statistics* 2014; 23(4): 1126–1142.

38. van den Boom W, Tallarita M and De Iorio M. Bayesian joint modelling of recurrence and survival: a conditional approach, 2020. arXiv:2005.06819v1.

39. Bouanani FE and Ben-Azza H. Efficient performance evaluation for EGC, MRC and SC receivers over Weibull multipath fading channel. In *Lecture Notes of the Institute for Computer Sciences, Social Informatics and Telecommunications Engineering*. Springer International Publishing, 2015. pp. 346–357. DOI:10.1007/978-3-319-24540-9_28.

Supplemental material for "Bayesian inference on the number of recurrent events: A joint model of recurrence and survival" by Willem van den Boom, Maria De Iorio and Marta Tallarita

S1   Gibbs sampler

This appendix describes the Gibbs sampler summarized in Algorithm S1.

S1.1   Normalization constant in $p(\boldsymbol{Y}_i, S_i \mid \text{---})$

The distribution $p(\boldsymbol{Y}_i, S_i \mid \text{---})$ defined in (2) is truncated by $T_{iN_i} \leq S_i$. Thus, the normalization constant of $p(\boldsymbol{Y}_i, S_i \mid \text{---})$ depends on parameters of interest and is thus required to be able to

---

Algorithm S1 Gibbs sampler

For each iteration of the Gibbs sampler:

1. For $k = 1, \ldots, q$, update β_k and γ_k by slice sampling with (S6) and (S9).

2. For each censored individual i:

    (a) Update N_i and $Y_{i(n_i+1)}^{N_i}$ using the reversible jump sampler from Section S1.3.

    (b) For $j = n_i + 1, \ldots, N_i$, sample Y_{ij} from (S10) truncated by $T_{i(n_i+1)} > c_i$ and $T_{iN_i} \leq S_i$ using the inverse transformation method.

    (c) Sample S_i from (S7) truncated by $S_i > \max(c_i, T_{iN_i})$ using the inverse transformation method.

3. Update $\boldsymbol{m}_i$ and δ_i for $i = 1, \ldots, L$ via Algorithm 8 from Neal (2000) using slice sampling with (S11–S13).

4. Sample M from the distribution in Equation 13 from Escobar and West (1995).

5. Update σ^2, η^2, r and λ by slice sampling with (S14–S16).

---

sample from the full conditionals of these parameters. This differs from previous likelihood specifications with log-normally distributed gap times (Aalen and Husebye, 1991; Paulon et al., 2018; Tallarita et al., 2020) because $p(\boldsymbol{Y}_i \mid \boldsymbol{\beta}, \boldsymbol{m}_i, N_i, S_i, \sigma^2, \boldsymbol{x}_i)$ is conditional on the number of events N_i.

To derive the normalization constant of $p(\boldsymbol{Y}_i, S_i \mid —)$, note that by (3)

$$f(\boldsymbol{Y}_i \mid \boldsymbol{\beta}, \boldsymbol{m}_i, N_i, \sigma^2, \boldsymbol{x}_i) = \mathcal{N}_{N_i}(\boldsymbol{Y}_i \mid \boldsymbol{\mu}_{\boldsymbol{Y}_i}, \boldsymbol{\Sigma}_{\boldsymbol{Y}_i}), \tag{S1}$$

where $\boldsymbol{\mu}_{\boldsymbol{Y}_i} = (\boldsymbol{x}_i^T \boldsymbol{\beta} + m_{i1}) \mathbf{1}_{N_i \times 1}$ and the $N_i \times N_i$ matrix $\boldsymbol{\Sigma}_{\boldsymbol{Y}_i}$ is defined by its tridiagonal inverse $\boldsymbol{\Sigma}_{\boldsymbol{Y}_i}^{-1}$ with $(\boldsymbol{\Sigma}_{\boldsymbol{Y}_i}^{-1})_{jj} = (m_{i2}^2 + 1)/\sigma^2$ for $j = 1, \ldots, N_i - 1$, $(\boldsymbol{\Sigma}_{\boldsymbol{Y}_i}^{-1})_{N_i N_i} = 1/\sigma^2$ and $(\boldsymbol{\Sigma}_{\boldsymbol{Y}_i}^{-1})_{j_1 j_2} = -m_{i2}/\sigma^2$ for $|j_1 - j_2| = 1$.[1] Consider now the untruncated $\boldsymbol{Y}_i^* \sim \mathcal{N}_{N_i}(\boldsymbol{\mu}_{\boldsymbol{Y}_i}, \boldsymbol{\Sigma}_{\boldsymbol{Y}_i})$ and define $T_{iN_i}^* = \sum_{j=1}^{N_i} e^{Y_{ij}^*}$. Similarly, define an untruncated and independent S_i^* by

$$\log(S_i^*) \sim \mathcal{N}\left\{ \boldsymbol{x}_i^T \boldsymbol{\gamma} + \delta_i, \eta^2 \right\} \tag{S2}$$

based on (4). Then, the normalization constant of $p(\boldsymbol{Y}_i, S_i \mid —)$ equals $\Pr(T_{iN_i}^* \leq S_i^*)$ where we drop the conditioning on $\boldsymbol{\beta}$, $\boldsymbol{\gamma}$, $\boldsymbol{m}_i$, δ_i, N_i, σ^2 and η^2 for notational convenience. For $N_i = 0$, $T_{iN_i}^* = T_{i0}^* = 0$ such that $\Pr(T_{iN_i}^* \leq S_i^*) = 1$. Therefore, the remainder of this subsection considers only $N_i \geq 1$. $T_{iN_i}^*$ is the sum of log-normal random variables. The distribution of such sums and $\Pr(T_{iN_i}^* \leq S_i^*)$ have no closed-form expression (Asmussen et al., 2019), requiring us to resort to approximations.

It is infeasible to evaluate $\Pr(T_{iN_i}^* \leq S_i^*)$ by numerical integration using quadrature for the values of N_i that we encounter. Fortunately, there is a literature on approximating $\Pr(T_{iN_i}^* \leq s)$ for fixed s (Botev et al., 2019, and references therein) which includes deterministic and Monte Carlo methods. As we aim to sample from the full conditionals of $\boldsymbol{\beta}$, $\boldsymbol{\gamma}$, $\boldsymbol{m}_i$, δ_i, N_i, σ^2 and η^2 as part of a Gibbs sampler, we need to evaluate the normalization constant $\Pr(T_{iN_i}^* \leq S_i^*)$ many times, requiring a fast approximation. We therefore choose the Fenton-Wilkinson method (Fenton, 1960) which approximates the distribution of $T_{iN_i}^*$ by a log-normal distribution with matched mean and variance. Asmussen et al. (2019) state that this approximation can be inaccurate for small N_i and when the elements in $\boldsymbol{Y}_i^*$ are dependent. However, their numerical results indicate good performance of the Fenton-Wilkinson method under these circumstances. Other fast approximations such as the saddle-point method from Asmussen et al. (2016) might be much more accurate, though they are also more complex than the Fenton-Wilkinson method.

For any matrix $\boldsymbol{A}$, denote the elementwise exponential by $e^{\boldsymbol{A}}$. Define $\text{diag}(\boldsymbol{\Sigma}_{\boldsymbol{Y}_i}) = \{(\boldsymbol{\Sigma}_{\boldsymbol{Y}_i})_{11}, \ldots, (\boldsymbol{\Sigma}_{\boldsymbol{Y}_i})_{N_i N_i}\}^T$. For any vector $\boldsymbol{a}$, denote the outer product with itself by $\boldsymbol{a}^{2\otimes} = \boldsymbol{a}\boldsymbol{a}^T$. Then,

$$\text{E}(e^{\boldsymbol{Y}_i^*}) = e^{\boldsymbol{\mu}_{\boldsymbol{Y}_i} + \text{diag}(\boldsymbol{\Sigma}_{\boldsymbol{Y}_i})/2} \qquad\qquad = e^{\boldsymbol{x}_i^T \boldsymbol{\beta} + m_{i1}} e^{\text{diag}(\boldsymbol{\Sigma}_{\boldsymbol{Y}_i})/2},$$
$$\text{Cov}(e^{\boldsymbol{Y}_i^*}) = \text{E}(e^{\boldsymbol{Y}_i^*})^{2\otimes} \circ (e^{\boldsymbol{\Sigma}_{\boldsymbol{Y}_i}} - \mathbf{1}_{N_i \times N_i}) = e^{2(\boldsymbol{x}_i^T \boldsymbol{\beta} + m_{i1})} \{e^{\text{diag}(\boldsymbol{\Sigma}_{\boldsymbol{Y}_i})/2}\}^{2\otimes} \circ (e^{\boldsymbol{\Sigma}_{\boldsymbol{Y}_i}} - \mathbf{1}_{N_i \times N_i});$$

---

[1]This implies $(\boldsymbol{\Sigma}_{\boldsymbol{Y}_i})_{j_1 j_2} = (m_{i2}^{|j_1 - j_2|} - m_{i2}^{j_1 + j_2})/(1 - m_{i2}^2)$ for $j_1, j_2 = 1, \ldots, N_i$.

where '∘' denotes the Hadamard product (Halliwell, 2015). Since $T_{iN_i}^* = \mathbf{1}_{1 \times N_i} \, e^{\boldsymbol{Y}_i^*}$,

$$
\begin{aligned}
\mathrm{E}(T_{iN_i}^*) &= \mathbf{1}_{1 \times N_i} \, \mathrm{E}(e^{\boldsymbol{Y}_i^*}) = e^{\boldsymbol{x}_i^T \boldsymbol{\beta} + m_{i1}} \, \mathrm{sum}\{e^{\mathrm{diag}(\boldsymbol{\Sigma}_{\boldsymbol{Y}_i})/2}\}, \\
\mathrm{Var}(T_{iN_i}^*) &= \mathbf{1}_{1 \times N_i} \, \mathrm{Cov}(e^{\boldsymbol{Y}_i^*}) \, \mathbf{1}_{N_i \times 1} \\
&= e^{2(\boldsymbol{x}_i^T \boldsymbol{\beta} + m_{i1})} \, \mathrm{sum}[\{e^{\mathrm{diag}(\boldsymbol{\Sigma}_{\boldsymbol{Y}_i})/2}\}^{2\otimes} \circ (e^{\boldsymbol{\Sigma}_{\boldsymbol{Y}_i}} - \mathbf{1}_{N_i \times N_i})];
\end{aligned}
\tag{S3}
$$

where $\mathrm{sum}(\cdot)$ denotes the grand sum of a matrix which is the sum of all its elements. The Fenton-Wilkinson approximation to the distribution of $T_{iN_i}^*$ is a log-normal distribution with the same mean and variance. Let $\hat{T}_{iN_i}^*$ be distributed according to this log-normal distribution. Then, $\log(\hat{T}_{iN_i}^*) \sim \mathcal{N}[\log\{\mathrm{E}(T_{iN_i}^*)\} - A, \, 2A]$ with

$$
\begin{aligned}
A &= \frac{1}{2} \log \left\{ 1 + \frac{\mathrm{Var}(T_{iN_i}^*)}{\mathrm{E}(T_{iN_i}^*)^2} \right\} \\
&= \frac{1}{2} \log(\mathrm{sum}[\{e^{\mathrm{diag}(\boldsymbol{\Sigma}_{\boldsymbol{Y}_i})/2}\}^{2\otimes} \circ e^{\boldsymbol{\Sigma}_{\boldsymbol{Y}_i}}]) - \log[\mathrm{sum}\{e^{\mathrm{diag}(\boldsymbol{\Sigma}_{\boldsymbol{Y}_i})/2}\}] \\
&= \frac{\mathrm{LS}_2}{2} - \mathrm{LS}_1,
\end{aligned}
$$

where the second equality follows from (S3) and $\mathrm{sum}\{e^{\mathrm{diag}(\boldsymbol{\Sigma}_{\boldsymbol{Y}_i})/2}\}^2 = \mathrm{sum}[\{e^{\mathrm{diag}(\boldsymbol{\Sigma}_{\boldsymbol{Y}_i})/2}\}^{2\otimes}]$, and $\mathrm{LS}_1 = \log[\mathrm{sum}\{e^{\mathrm{diag}(\boldsymbol{\Sigma}_{\boldsymbol{Y}_i})/2}\}]$ and $\mathrm{LS}_2 = \log(\mathrm{sum}[\{e^{\mathrm{diag}(\boldsymbol{\Sigma}_{\boldsymbol{Y}_i})/2}\}^{2\otimes} \circ e^{\boldsymbol{\Sigma}_{\boldsymbol{Y}_i}}])$ are introduced for notational convenience. Moreover, by standard properties of the Gaussian distribution, the independence of $\hat{T}_{iN_i}^*$ and S_i^* and (S2),

$$
\log(\hat{T}_{iN_i}^*) - \log(S_i^*) \sim \mathcal{N}[\log\{\mathrm{E}(T_{iN_i}^*)\} - A - \boldsymbol{x}_i^T \boldsymbol{\gamma} - \delta_i, \, 2A + \eta^2].
$$

Our approximation to the normalization constant is thus

$$
\begin{aligned}
\mathrm{Pr}(T_{iN_i}^* \leq S_i^*) &\approx \mathrm{Pr}\{\hat{T}_{iN_i}^* \leq S_i^*\} = \mathrm{Pr}\{\log(\hat{T}_{iN_i}^*) - \log(S_i^*) \leq 0\} \\
&= \Phi\left[\frac{-\log\{\mathrm{E}(T_{iN_i}^*)\} + A + \boldsymbol{x}_i^T \boldsymbol{\gamma} + \delta_i}{\sqrt{2A + \eta^2}} \right] \\
&= \Phi\left\{ \frac{-\boldsymbol{x}_i^T \boldsymbol{\beta} - m_{i1} - 2\,\mathrm{LS}_1 + \mathrm{LS}_2/2 + \boldsymbol{x}_i^T \boldsymbol{\gamma} + \delta_i}{\sqrt{\mathrm{LS}_2 - 2\,\mathrm{LS}_1 + \eta^2}} \right\},
\end{aligned}
$$

where $\Phi(\cdot)$ is the cumulative density function of $\mathcal{N}(0, 1)$ and the last equality follows from (S3). In the remainder of this appendix, we write $\mathrm{Pr}(T_{iN_i}^* \leq S_i^*)$ even though we use this approximation.

LS_1 and LS_2 only depend on $\boldsymbol{\Sigma}_{\boldsymbol{Y}_i}$. Therefore, we only need to recompute LS_1 and LS_2 in the Gibbs sampler when $\boldsymbol{\Sigma}_{\boldsymbol{Y}_i}$, which is a function of m_{i2}, σ^2 and N_i, changes.

S1.2 Regression coefficients

The full conditional for $\boldsymbol{\beta}$ follows from the prior and the likelihood in Section 2.2 as

$$
p(\boldsymbol{\beta} \mid -) \propto \mathcal{N}_q(\boldsymbol{\beta} \mid 0, \sigma_\beta^2 \boldsymbol{I}_q) \prod_{i=1}^{L} p(\boldsymbol{Y}_i, S_i \mid -).
\tag{S4}
$$

3

We can use the expression for $f(\boldsymbol{Y}_i \mid \boldsymbol{\beta}, \boldsymbol{m}_i, N_i, \sigma^2, \boldsymbol{x}_i)$ in (3) or (S1) directly to evaluate (S4), but that is computationally expensive as it involves a multitude of Gaussian density evaluations. Instead, we introduce $Y_{i1}^{\boldsymbol{\beta}} = Y_{i1} - m_{i1}$, $Y_{ij}^{\boldsymbol{\beta}} = \{Y_{ij} - m_{i1} - m_{i2}(Y_{i(j-1)} - m_{i1})\}/(1 - m_{i2})$ for $j = 2, \ldots, N_i$ and the $N_i \times N_i$ diagonal matrix $\boldsymbol{\Sigma}_{\boldsymbol{\beta},i}$ with $\mathrm{diag}(\boldsymbol{\Sigma}_{\boldsymbol{\beta},i}) = \sigma^2 \{1, (1 - m_{i2})^{-2}, \ldots, (1 - m_{i2})^{-2}\}^T$. Then, we can rewrite (3) as

$$f(\boldsymbol{Y}_i \mid \boldsymbol{\beta}, \boldsymbol{m}_i, N_i, \sigma^2, \boldsymbol{x}_i) = \mathcal{N}_{N_i}(\boldsymbol{Y}_i^{\boldsymbol{\beta}} \mid \boldsymbol{1}_{N_i \times 1}\, \boldsymbol{x}_i^T \boldsymbol{\beta}, \boldsymbol{\Sigma}_{\boldsymbol{\beta},i}), \quad T_{iN_i} \leq S_i.$$

Inserting this expression into (S4) yields a normal-normal model such that

$$p(\boldsymbol{\beta} \mid -) \propto \frac{\mathcal{N}_q(\boldsymbol{\beta} \mid \boldsymbol{\mu}_{\boldsymbol{\beta}}^*, \boldsymbol{\Sigma}_{\boldsymbol{\beta}}^*)}{\prod_{i=1}^{L} \Pr(T_{iN_i}^* \leq S_i^*)}, \tag{S5}$$

where $\boldsymbol{\mu}_{\boldsymbol{\beta}}^* = \boldsymbol{\Sigma}_{\boldsymbol{\beta}}^* \sum_{i=1}^{L} \boldsymbol{x}_i \boldsymbol{1}_{1 \times N_i} \boldsymbol{\Sigma}_{\boldsymbol{\beta},i}^{-1} \boldsymbol{Y}_i^{\boldsymbol{\beta}}$, and $\boldsymbol{\Sigma}_{\boldsymbol{\beta}}^* = \{\boldsymbol{I}_q/\sigma_\beta^2 + \sum_{i=1}^{L} \mathrm{sum}(\boldsymbol{\Sigma}_{\boldsymbol{\beta},i}^{-1})\, \boldsymbol{x}_i \boldsymbol{x}_i^T\}^{-1}$ with $\mathrm{sum}(\boldsymbol{\Sigma}_{\boldsymbol{\beta},i}^{-1}) = \{1 + (N_i - 1)(1 - m_{i2})^2\}/\sigma^2$ for $N_i \geq 1$ and $\mathrm{sum}(\boldsymbol{\Sigma}_{\boldsymbol{\beta},i}^{-1}) = 0$ for $N_i = 0$. Recalling the conditional distributions of a multivariate normal, we obtain

$$p(\beta_k \mid -) \propto \frac{\mathcal{N}(\beta_k \mid \mu_{\beta_k}^*, \Sigma_{\beta_k}^*)}{\prod_{i=1}^{L} \Pr(T_{iN_i}^* \leq S_i^*)}, \tag{S6}$$

where $\mu_{\beta_k}^* = (\boldsymbol{\mu}_{\boldsymbol{\beta}}^*)_k + (\boldsymbol{\Sigma}_{\boldsymbol{\beta}}^*)_{k,-k}(\boldsymbol{\Sigma}_{\boldsymbol{\beta}}^*)_{-k,-k}^{-1}\{\boldsymbol{\beta}_{-k} - (\boldsymbol{\mu}_{\boldsymbol{\beta}}^*)_{-k}\}$ and $\Sigma_{\beta_k}^* = (\boldsymbol{\Sigma}_{\boldsymbol{\beta}}^*)_{kk} - (\boldsymbol{\Sigma}_{\boldsymbol{\beta}}^*)_{k,-k}(\boldsymbol{\Sigma}_{\boldsymbol{\beta}}^*)_{-k,-k}^{-1}(\boldsymbol{\Sigma}_{\boldsymbol{\beta}}^*)_{k,-k}^T$ with the $1 \times (q-1)$ row vector $(\boldsymbol{\Sigma}_{\boldsymbol{\beta}}^*)_{k,-k}$ equal to the kth row of $\boldsymbol{\Sigma}_{\boldsymbol{\beta}}^*$ without its kth element, the $(q-1) \times (q-1)$ matrix $(\boldsymbol{\Sigma}_{\boldsymbol{\beta}}^*)_{-k,-k}$ equal to $\boldsymbol{\Sigma}_{\boldsymbol{\beta}}^*$ without its kth row and kth column, and $\boldsymbol{a}_{-k}$ equal to the vector $\boldsymbol{a}$ without its kth element, for $k = 1, \ldots, q$. Now, the Gibbs update for $\boldsymbol{\beta}$ follows as slice sampling with (S6) as target density for $k = 1, \ldots, q$.

For the other regression coefficient $\boldsymbol{\gamma}$, consider (2) and (4) such that

$$f\{\log(S_i) \mid -\} \propto \mathcal{N}\{\log(S_i) \mid \boldsymbol{x}_i^T \boldsymbol{\gamma} + \delta_i, \eta^2\}, \quad S_i \geq T_{iN_i}. \tag{S7}$$

The full conditional for $\boldsymbol{\gamma}$ then follows with the prior $\boldsymbol{\gamma} \sim \mathcal{N}_q(0, \sigma_\gamma^2 \boldsymbol{I}_q)$ from Section 2.3 as

$$p(\boldsymbol{\gamma} \mid -) \propto \mathcal{N}_q(\boldsymbol{\gamma} \mid 0, \sigma_\gamma^2 \boldsymbol{I}_q) \prod_{i=1}^{L} p\{\log(S_i) \mid -\} \propto \frac{\mathcal{N}_q(\boldsymbol{\gamma} \mid \boldsymbol{\mu}_{\boldsymbol{\gamma}}^*, \boldsymbol{\Sigma}_{\boldsymbol{\gamma}}^*)}{\prod_{i=1}^{L} \Pr(T_{iN_i}^* \leq S_i^*)} \tag{S8}$$

where $\boldsymbol{\mu}_{\boldsymbol{\gamma}}^* = \boldsymbol{\Sigma}_{\boldsymbol{\gamma}}^* \boldsymbol{X}^T(\boldsymbol{U} - \boldsymbol{\delta})/\eta^2$ and $\boldsymbol{\Sigma}_{\boldsymbol{\gamma}}^* = (\boldsymbol{I}_q/\sigma_\gamma^2 + \boldsymbol{X}^T \boldsymbol{X}/\eta^2)^{-1}$ with the $L \times q$ matrix $\boldsymbol{X} = (\boldsymbol{x}_1, \ldots, \boldsymbol{x}_L)^T$ and the L-dimensional vector $\boldsymbol{U} = \{\log(S_1), \ldots, \log(S_L)\}^T$. Analogously to (S6), we obtain

$$p(\gamma_k \mid -) \propto \frac{\mathcal{N}(\gamma_k \mid \mu_{\gamma_k}^*, \Sigma_{\gamma_k}^*)}{\prod_{i=1}^{L} \Pr(T_{iN_i}^* \leq S_i^*)}, \tag{S9}$$

where $\mu_{\gamma_k}^* = (\boldsymbol{\mu}_{\boldsymbol{\gamma}}^*)_k + (\boldsymbol{\Sigma}_{\boldsymbol{\gamma}}^*)_{k,-k}(\boldsymbol{\Sigma}_{\boldsymbol{\gamma}}^*)_{-k,-k}^{-1}\{\boldsymbol{\gamma}_{-k} - (\boldsymbol{\mu}_{\boldsymbol{\gamma}}^*)_{-k}\}$ and $\Sigma_{\gamma_k}^* = (\boldsymbol{\Sigma}_{\boldsymbol{\gamma}}^*)_{kk} - (\boldsymbol{\Sigma}_{\boldsymbol{\gamma}}^*)_{k,-k}(\boldsymbol{\Sigma}_{\boldsymbol{\gamma}}^*)_{-k,-k}^{-1}(\boldsymbol{\Sigma}_{\boldsymbol{\gamma}}^*)_{k,-k}^T$. Similarly to $\boldsymbol{\beta}$, the Gibbs update for $\boldsymbol{\gamma}$ follows as slice sampling with (S9) as target density for $k = 1, \ldots, q$.

S1.3 Reversible jump sampler for N_i

If individual i is censored, then the number of events N_i is unknown and object of inference. Since N_i affects the dimensionality of $\boldsymbol{Y}_i$, we use a reversible jump sampler (Green, 1995; Waagepetersen and Sorensen, 2001) to update it. The sampler updates N_i and $Y_{i(n_i+1)}^{N_i} = (Y_{i(n_i+1)}, \ldots, Y_{iN_i})^T$ jointly. It is a Metropolis-Hastings algorithm on a state space of varying dimension. The state space is $\bigcup_{N_i=n_i}^{\infty} \mathbb{R}^{N_i-n_i}$ in our case.

The proposal distribution for N_i and $Y_{i(n_i+1)}^{N_i}$ is as follows. Since $N_i \geq n_i$, we sample $N_i \sim \mathbb{1}_{[n_i,\infty)} \operatorname{NegBin}(r, \lambda)$, a negative binomial truncated to $[n_i, \infty)$, using the inverse transformation method. To complete the joint proposal, we only need to specify the proposal distribution of $Y_{i(n_i+1)}^{N_i}$ given N_i. We use $T_{i(n_i+1)} \sim \mathcal{U}(c_i, S_i)$ and $T_{ij} \mid T_{i(j-1)} \sim \mathcal{U}(T_{i(j-1)}, S_i)$ for $j = n_i + 2, \ldots, N_i$ as $T_{iN_i} \leq S_i$. We prefer this proposal over sampling along the lines of (3) as then the proposal density would involve an intractable normalization constant similarly to (2). Instead, we now have $\Pr(T_{i(n_i+1)} \leq t) = (t - c_i)/(S_i - c_i)$ and $\Pr(T_{ij} \leq t \mid T_{i(j-1)}) = (t - T_{i(j-1)})/(S_i - T_{i(j-1)})$ for $j = n_i + 2, \ldots, N_i$. Inserting (1) shows $\Pr(Y_{i(n_i+1)} \leq y) = (e^y + T_{in_i} - c_i)/(S_i - c_i)$ and $\Pr(Y_{ij} \leq y \mid T_{i(j-1)}) = e^y/(S_i - T_{i(j-1)})$ for $j = n_i + 2, \ldots, N_i$. The proposal density is thus

$$f_{N_i}(Y_{i(n_i+1)}^{N_i}) = \begin{cases} \frac{e^{Y_{i(n_i+1)}+T_{n_i}-c_i}}{S_i-c_i} \prod_{j=n_i+2}^{N_i} \frac{e^{Y_{ij}}}{S_i-T_{i(j-1)}}, & N_i > n_i \\ 1, & N_i = n_i \end{cases}.$$

To derive the acceptance probability, we follow the notation in Waagepetersen and Sorensen (2001, Section 4) where proposed values are denoted by a prime ('). Specifically, the proposal distributions are written as $p_{N_iN_i'} \propto \mathbb{1}[N_i' \geq n_i] \operatorname{NegBin}(N_i' \mid r, \lambda)$ and $q_{N_iN_i'}(Y_{i(n_i+1)}^{N_i}, \cdot) = f_{N_i'}(\cdot)$. The target density follows from Sections 2.1, 2.2 and S1.1 as

$$\pi(N_i, Y_{i(n_i+1)}^{N_i}) \propto \operatorname{NegBin}(N_i \mid r, \lambda) \times \begin{cases} 1, & N_i = 0 \\ \frac{f(\boldsymbol{Y}_i \mid \boldsymbol{\beta}, \boldsymbol{m}_i, N_i, \sigma^2, \boldsymbol{x}_i)}{\Pr(T_{iN_i}^* \leq S_i^*)}, & N_i \geq 1 \end{cases}$$

for $N_i \geq n_i$, $T_{i(n_i+1)} > c_i$ and $T_{iN_i} \leq S_i$, and where $f(\boldsymbol{Y}_i \mid \boldsymbol{\beta}, \boldsymbol{m}_i, N_i, \sigma^2, \boldsymbol{x}_i)$ is given by (3). The dimension changing map can be written in the notation of Waagepetersen and Sorensen (2001, Section 4) as

$$g_{N_iN_i'}\{Y_{i(n_i+1)}^{N_i}, (Y')_{i(n_i+1)}^{N_i'}\} = \begin{pmatrix} g_{1N_iN_i'}\{Y_{i(n_i+1)}^{N_i}, (Y')_{i(n_i+1)}^{N_i'}\} \\ g_{2N_iN_i'}\{Y_{i(n_i+1)}^{N_i}, (Y')_{i(n_i+1)}^{N_i'}\} \end{pmatrix},$$

where $g_{1N_iN_i'}\{Y_{i(n_i+1)}^{N_i}, (Y')_{i(n_i+1)}^{N_i'}\} = (Y')_{i(n_i+1)}^{N_i'}$ and $g_{2N_iN_i'}\{Y_{i(n_i+1)}^{N_i}, (Y')_{i(n_i+1)}^{N_i'}\} = Y_{i(n_i+1)}^{N_i}$. The acceptance probability is then given by (Waagepetersen and Sorensen, 2001, Equation 19)

$$a_{N_iN_i'}\{Y_{i(n_i+1)}^{N_i}, (Y')_{i(n_i+1)}^{N_i'}\}$$
$$= \min\left[1, \frac{\pi\{N_i', (Y')_{i(n_i+1)}^{N_i'}\}\, p_{N_i'N_i}\, q_{N_i'N_i}\{(Y')_{i(n_i+1)}^{N_i'}, Y_{i(n_i+1)}^{N_i}\}}{\pi(N_i, Y_{i(n_i+1)}^{N_i})\, p_{N_iN_i'}\, q_{N_iN_i'}\{Y_{i(n_i+1)}^{N_i}, (Y')_{i(n_i+1)}^{N_i'}\}} \, |J_{g_{N_iN_i'}}|\right],$$

where $|J_{g_{N_i N_i'}}|$ denotes the absolute value of the determinant of the Jacobian of $g_{N_i N_i'}$. The elements of $J_{g_{N_i N_i'}}$ are all zero except for one entry in each row that equals one so that the absolute value of its determinant equals one. Additionally substituting the definitions of the various terms yields as acceptance probability

$$a_{N_i N_i'}\{Y_{i(n_i+1)}^{N_i}, (Y')_{i(n_i+1)}^{N_i'}\} = \min\left[1, \frac{C_{N_i'}\{(Y')_{i(n_i+1)}^{N_i'}\}}{C_{N_i}(Y_{i(n_i+1)}^{N_i})} \times \frac{f_{N_i}(Y_{i(n_i+1)}^{N_i})}{f_{N_i'}\{(Y')_{i(n_i+1)}^{N_i'}\}}\right],$$

where

$$C_{N_i}(Y_{i(n_i+1)}^{N_i}) = \begin{cases} 1, & N_i = 0 \\ \frac{f(\mathbf{Y}_i|\boldsymbol{\beta},\mathbf{m}_i,N_i,\sigma^2,\mathbf{x}_i)}{\Pr(T_{iN_i}^* \leq S_i^*)}, & N_i \geq 1 \end{cases}.$$

This reversible jump sampler updates both N_i and $Y_{i(n_i+1)}^{N_i}$. Additionally, we update $Y_{i(n_i+1)}^{N_i}$ as described in the next section to improve mixing of the Gibbs sampler in case the Metropolis-Hastings sampler in this section rarely accepts the proposed samples.

S1.4   Survival and log gap times

If individual i is censored, then the log gap times $Y_{i(n_i+1)}^{N_i}$ and the survival time S_i are imputed in the Gibbs sampler. The full conditional for the vector $Y_{i(n_i+1)}^{N_i}$ is hard to sample from due to the truncation $T_{iN_i} \leq S_i$. Instead, we consider its elementwise full conditionals. By (2) and (3), for $j = 2, \ldots, N_i - 1$,

$$p(Y_{i1} \mid -) \propto \begin{cases} \mathcal{N}(Y_{i1} \mid \boldsymbol{x}_i^T\boldsymbol{\beta} + m_{i1}, \sigma^2), & N_i = 1, \\ \mathcal{N}\left\{Y_{i1} \mid \boldsymbol{x}_i^T\boldsymbol{\beta} + m_{i1} + \frac{m_{i2}}{1+m_{i2}^2}(Y_{i2} - \boldsymbol{x}_i^T\boldsymbol{\beta} - m_{i1}), \frac{\sigma^2}{1+m_{i2}^2}\right\}, & N_i \geq 2, \end{cases}$$

$$p(Y_{ij} \mid -) \propto \mathcal{N}\left\{Y_{ij} \mid \boldsymbol{x}_i^T\boldsymbol{\beta} + m_{i1} + \frac{m_{i2}}{1+m_{i2}^2}(Y_{i(j-1)} + Y_{i(j+1)} - 2\boldsymbol{x}_i^T\boldsymbol{\beta} - 2m_{i1}), \frac{\sigma^2}{1+m_{i2}^2}\right\},$$

$$p(Y_{iN_i} \mid -) \propto \mathcal{N}\{Y_{iN_i} \mid \boldsymbol{x}_i^T\boldsymbol{\beta} + m_{i1} + m_{i2}(Y_{i(N_i-1)} - \boldsymbol{x}_i^T\boldsymbol{\beta} - m_{i1}), \sigma^2\}, \quad N_i \geq 2;$$
(S10)

for $T_{i(n_i+1)} > c_i$ and $T_{iN_i} \leq S_i$. Let $R_{ij} = S_i - T_{iN_i} + e^{Y_{ij}} = S_i - \sum_{j^* \neq j} e^{Y_{ij^*}}$. Then, $e^{Y_{ij}}$ is bounded from above by R_{ij} since $T_{iN_i} \leq S_i$. Additionally, $e^{Y_{i(n_i+1)}}$ is bounded from below by $c_i - T_{in_i}$ since $T_{i(n_i+1)} > c_i$. Therefore, we can sample from (S10) with these truncations for $j = n_i + 1, \ldots, N_i$ using the inverse transform method.

We sample S_i from (S7) truncated to $S_i > c_i$ using the inverse transform method.

S1.5   Dirichlet process parameters

As detailed in Section 1, the discreteness of the DP induces clustering of the individuals. Denote the random effects in the hth cluster by $(\boldsymbol{m}_h^*, \delta_h^*)$ and the cluster that individual i belongs to by s_i. Then, $s_i = h$ if and only if $(\boldsymbol{m}_i, \delta_i) = (\boldsymbol{m}_h^*, \delta_h^*)$. To update $(\boldsymbol{m}_i, \delta_i)$ for $i = 1, \ldots, L$, we update the cluster allocations s_i and the cluster-specific parameters $(\boldsymbol{m}_h^*, \delta_h^*)$,

6

using Algorithm 8 from Neal (2000) with the algorithm-specific parameter $m = 2$. We choose this algorithm since independent sampling from the full conditional of $\boldsymbol{m}_h^*$, required for instance for Neal's Algorithm 2, is hard due to the intractability of the likelihood discussed in Section S1.1.

Neal's Algorithm 8 requires sampling of $(\boldsymbol{m}_h^*, \delta_h^*)$ that leaves its full conditional distribution invariant. We do this by first sampling m_{h1}^*, then m_{h2}^* and lastly δ_h^* such that their respective full conditionals remain invariant. A derivation analogous to the one for (S5) yields the full conditional for m_{h1}^*. Specifically, we introduce $Y_{i1}^{m_{i1}} = Y_{i1} - \boldsymbol{x}_i^T\boldsymbol{\beta}$, $Y_{ij}^{m_{i1}} = \{Y_{ij} - \boldsymbol{x}_i^T\boldsymbol{\beta} - m_{i2}(Y_{i(j-1)} - \boldsymbol{x}_i^T\boldsymbol{\beta})\}/(1 - m_{i2})$ for $j = 2, \ldots, N_i$ and the $N_i \times N_i$ diagonal matrix $\boldsymbol{\Sigma}_{m_{i1}}$ with $\text{diag}(\boldsymbol{\Sigma}_{m_{i1}}) = \sigma^2 \{1, (1 - m_{i2})^{-2}, \ldots, (1 - m_{i2})^{-2}\}^T$. Then,

$$p(m_{h1}^* \mid —) \propto \frac{\mathcal{N}(m_{h1}^* \mid \mu_{m_{h1}^*}^*, \Sigma_{m_{h1}^*}^*)}{\prod_{\{i|s_i=h\}} \Pr(T_{iN_i}^* \leq S_i^*)}, \tag{S11}$$

where $\mu_{m_{h1}^*}^* = \Sigma_{m_{h1}^*}^* \sum_{\{i|s_i=h\}} \mathbf{1}_{1 \times N_i} \boldsymbol{\Sigma}_{m_{i1}}^{-1} \boldsymbol{Y}_i^{m_{i1}}$ and $\Sigma_{m_{h1}^*}^* = 1/\{1/\sigma_m^2 + \sum_{\{i|s_i=h\}} \text{sum}(\boldsymbol{\Sigma}_{m_{i1}}^{-1})\}$ with $\text{sum}(\boldsymbol{\Sigma}_{m_{i1}}^{-1}) = \{1 + (N_i - 1)(1 - m_{i2})^2\}/\sigma^2$.

Similarly for m_{h2}^*, we introduce $Y_{i(j-1)}^{m_{i2}} = (Y_{ij} - \boldsymbol{x}_i^T\boldsymbol{\beta} - m_{i1})/(Y_{i(j-1)} - \boldsymbol{x}_i^T\boldsymbol{\beta} - m_{i1})$ for $j = 2, \ldots, N_i$ and the $(N_i-1) \times (N_i-1)$ diagonal matrix $\boldsymbol{\Sigma}_{m_{i2}}$ with $(\boldsymbol{\Sigma}_{m_{i2}})_{jj} = \sigma^2/(Y_{ij} - \boldsymbol{x}_i^T\boldsymbol{\beta} - m_{i1})^2$ for $j = 1, \ldots, N_i - 1$. Then,

$$p(m_{h2}^* \mid —) \propto \frac{\mathcal{N}(m_{h2}^* \mid \mu_{m_{h2}^*}^*, \Sigma_{m_{h2}^*}^*)}{\prod_{\{i|s_i=h\}} \Pr(T_{iN_i}^* \leq S_i^*)}, \tag{S12}$$

where $\mu_{m_{h2}^*}^* = \Sigma_{m_{h2}^*}^* \sum_{\{i|s_i=h\}} \mathbf{1}_{1 \times N_i} \boldsymbol{\Sigma}_{m_{i2}}^{-1} \boldsymbol{Y}_i^{m_{i2}}$ and $\Sigma_{m_{h2}^*}^* = 1/\{1/\sigma_m^2 + \sum_{\{i|s_i=h\}} \text{sum}(\boldsymbol{\Sigma}_{m_{i2}}^{-1})\}$ with $\text{sum}(\boldsymbol{\Sigma}_{m_{i2}}^{-1}) = \sum_{j=1}^{N_i-1}(Y_{ij} - \boldsymbol{x}_i^T\boldsymbol{\beta} - m_{i1})^2/\sigma^2$.

For δ_h^*, a derivation similar to the one for (S8) yields

$$p(\delta_h^* \mid —) \propto \frac{\mathcal{N}(\delta_h^* \mid \mu_{\delta_h^*}^*, \Sigma_{\delta_h^*}^*)}{\prod_{\{i|s_i=h\}} \Pr(T_{iN_i}^* \leq S_i^*)} \tag{S13}$$

where $\mu_{\delta_h^*}^* = \Sigma_{\delta_h^*}^* \sum_{\{i|s_i=h\}} \{\log(S_i) - \boldsymbol{x}_i^T\boldsymbol{\gamma}\}/\eta^2$ and $\Sigma_{\delta_h^*}^* = 1/(1/\sigma_\delta^2 + |\{i \mid s_i = h\}|/\eta^2)$. Now, the update of $(\boldsymbol{m}_h^*, \delta_h^*)$ follows as slice sampling with (S11–S13) as target density for $h = 1, \ldots, K$ where K is the number of clusters.

Equation 13 from Escobar and West (1995) provides the Gibbs update for the DP concentration parameter M: First, draw $\eta_M \sim \text{Beta}(M + 1, L)$. Then, with probability $1/[1 + L\{b_M - \log(\eta_M)\}/(a_M + K - 1)]$ where L denotes the number of individuals, draw $M \sim \text{Gamma}\{a_M + K, b_M - \log(\eta_M)\}$. Otherwise, draw $M \sim \text{Gamma}\{a_M + K - 1, b_M - \log(\eta_M)\}$.

S1.6 Variance parameters, r and λ

Recalling the prior and likelihood for σ^2 from Section 2.3 and (3), respectively, we obtain

$$p(\sigma^2 \mid —) \propto \frac{\text{Inv-Gamma}\{\sigma^2 \mid (\nu_{\sigma^2} + \sum_{i=1}^L N_i)/2, (\nu_{\sigma^2}\sigma_0^2 + \sum_{i=1}^L \|\boldsymbol{Y}_i - \boldsymbol{\mu}_i^{\sigma^2}\|^2)/2\}}{\prod_{i=1}^L \Pr(T_{iN_i}^* \leq S_i^*)}, \tag{S14}$$

where $\mu_{i1}^{\sigma^2} = \boldsymbol{x}_i^T \boldsymbol{\beta} + m_{i1}$ and $\mu_{ij}^{\sigma^2} = \boldsymbol{x}_i^T \boldsymbol{\beta} + m_{i1} + m_{i2}(Y_{i(j-1)} - \boldsymbol{x}_i^T \boldsymbol{\beta} - m_{i1})$ for $j = 2, \ldots, N_i$. Similarly for η^2, its prior from Section 2.3 and the likelihood in (S7) yield

$$p(\eta^2 \mid -) \propto \frac{\text{Inv-Gamma}\{\eta^2 \mid (\nu_{\eta^2} + L)/2, \, (\nu_{\eta^2}\,\eta_0^2 + \sum_{i=1}^{L}\{\log(S_i) - \boldsymbol{x}_i^T\boldsymbol{\gamma} - \delta_i\}^2)/2\}}{\prod_{i=1}^{L} \Pr(T_{iN_i}^* \le S_i^*)}.$$

(S15)

Now, the Gibbs updates for σ^2 and η^2 follow as slice sampling with (S14) and (S15) as target density, respectively.

The full conditionals for r and λ follow, up to proportionality, from their gamma priors in Section 2.3 and the negative binomial likelihood from Section 2.2,

$$p(\boldsymbol{N} \mid r, \lambda) = \prod_{i=1}^{L} \frac{\Gamma(N_i + r)}{\Gamma(r) N_i!} p(r, \lambda)^{N_i} \{1 - p(r, \lambda)\}^r,$$

(S16)

where $\Gamma(\cdot)$ is the gamma function and $p(r, \lambda) = \lambda/(\lambda + r)$. The updates for r and λ follow then as slice sampling with these full conditionals.

S2 Prior specification

For the application of our model to the AF data in Section S4, the hyperparameters of the prior distributions in Section 2.3 are chosen as follows. The hyperparameters of the priors on σ^2 and η^2 are such that their prior means equal 1 and their prior variances equal 100. Specifically,

$$\mathrm{E}(\sigma^2) = \frac{\nu_1\,\sigma_0^2/2}{\nu_1/2 - 1} = \frac{\nu_1\,\sigma_0^2}{\nu_1 - 2} = 1,$$

$$\mathrm{Var}(\sigma^2) = \frac{\nu_1^2\,\sigma_0^4/4}{(\nu_1/2 - 1)^2\,(\nu_1/2 - 2)} = \frac{2\,\nu_1^2\,\sigma_0^4}{(\nu_1 - 2)^2\,(\nu_1 - 4)} = 100,$$

$$\mathrm{E}(\eta^2) = \frac{\nu_2\,\eta_0^2/2}{\nu_2/2 - 1} = \frac{\nu_2\eta_0^2}{\nu_2 - 2} = 1,$$

$$\mathrm{Var}(\eta^2) = \frac{\nu_2^2\,\eta_0^4/4}{(\nu_2/2 - 1)^2\,(\nu_2/2 - 2)} = \frac{2\,\nu_2^2\,\eta_0^4}{(\nu_2 - 2)^2\,(\nu_2 - 4)} = 100;$$

yields $\nu_1 = 4.02$, $\sigma_0^2 = 2.02/4.02$, $\nu_2 = 4.02$ and $\eta_0^2 = 2.02/4.02$. Similarly, the prior variances of the elements of the regression coefficients $\boldsymbol{\beta}$ and $\boldsymbol{\gamma}$ equal $\sigma_\beta^2 = \sigma_\gamma^2 = 100$. The hyperparameters related to the base measure G_0 of the DP prior are chosen as non-informative with $\sigma_\delta^2 = \sigma_m^2 = 100$. We choose an uninformative prior on the DP concentration parameter M with $a_M = 2$ and $b_M = 1$. Finally, $a_r = b_r = a_\lambda = b_\lambda = 1$ specifies the priors for r and λ.

S3   Additional simulation studies

S3.1   Prior sensitivity study

This section considers the effect of choosing different hyperparameters a_λ and b_λ on the posterior inference for the number of recurrent events N_i. Specifically, consider the simulated data from Section 3 where 90% of the individuals are censored. Then, we run the Gibbs sampler with $a_\lambda = \mu_\lambda^2$ and $b_\lambda = \mu_\lambda$, such that $E(\lambda) = \mu_\lambda$ and $\text{Var}(\lambda) = 1$ a priori, for $\mu_\lambda = 0.1, 1, 10$ with the remainder of the set-up being the same as in Section 3.

Figure S1 shows the posterior inference on N_i analogously to Figure 1. The results do not vary notably across the different choices of prior mean μ_λ.

S3.2   Model misspecification

In Section 3, the data are simulated from the model in Section 2.2. Here, we consider data that are simulated from a different model. Specifically, we do not generate the survival times S_i from a log-normal distribution as per (4) but instead from a Gompertz distribution with shape parameter 0.01 and scale parameter $\exp(-\boldsymbol{x}_i^T \boldsymbol{\gamma} - \delta_i)$. Then, $E(S_i \mid \boldsymbol{\gamma}, \delta_i, \eta^2) = \exp(\boldsymbol{x}_i^T \boldsymbol{\gamma} + \delta_i + 1.41)$. Under the log-normal distribution in (4), we have $E(S_i \mid \boldsymbol{\gamma}, \delta_i, \eta^2) = \exp(\boldsymbol{x}_i^T \boldsymbol{\gamma} + \delta_i + \eta^2/2)$, such that the regression coefficients $\boldsymbol{\gamma}$ retain their interpretation under the misspecification using the Gompertz distribution as data generation process. The remainder of the set-up is the same as in Section 3.

Figures S2 through S6 present the results analogously to Figures 1 through 5. Posterior inference appears robust to the misspecification with the credible intervals for N_i mostly covering the true values (Figure S2) and the credible intervals for the regression coefficients all covering the true values (Figure S6). The posterior mode for the number of clusters is not equal to the true value of three in the absence of censored data (Figure S5). This is unsurprising as the Dirichlet process can accommodate any empirical distribution by adding further mixture components when necessary

S3.3   Bias and mean squared error of the posterior means

To assess the bias and the mean squared error (MSE) of the posterior means of our method, we repeat the simulation of Section 3 eight times. Then, we estimate the bias as the difference between the average of the resulting eight posterior means and the parameter values from which the data were generated. We compute the MSE analogously.

Table S1 contains the results. For those parameters for which the bias or MSE varies notably with the censoring level, we consistently see that higher censoring results in larger bias and MSE.
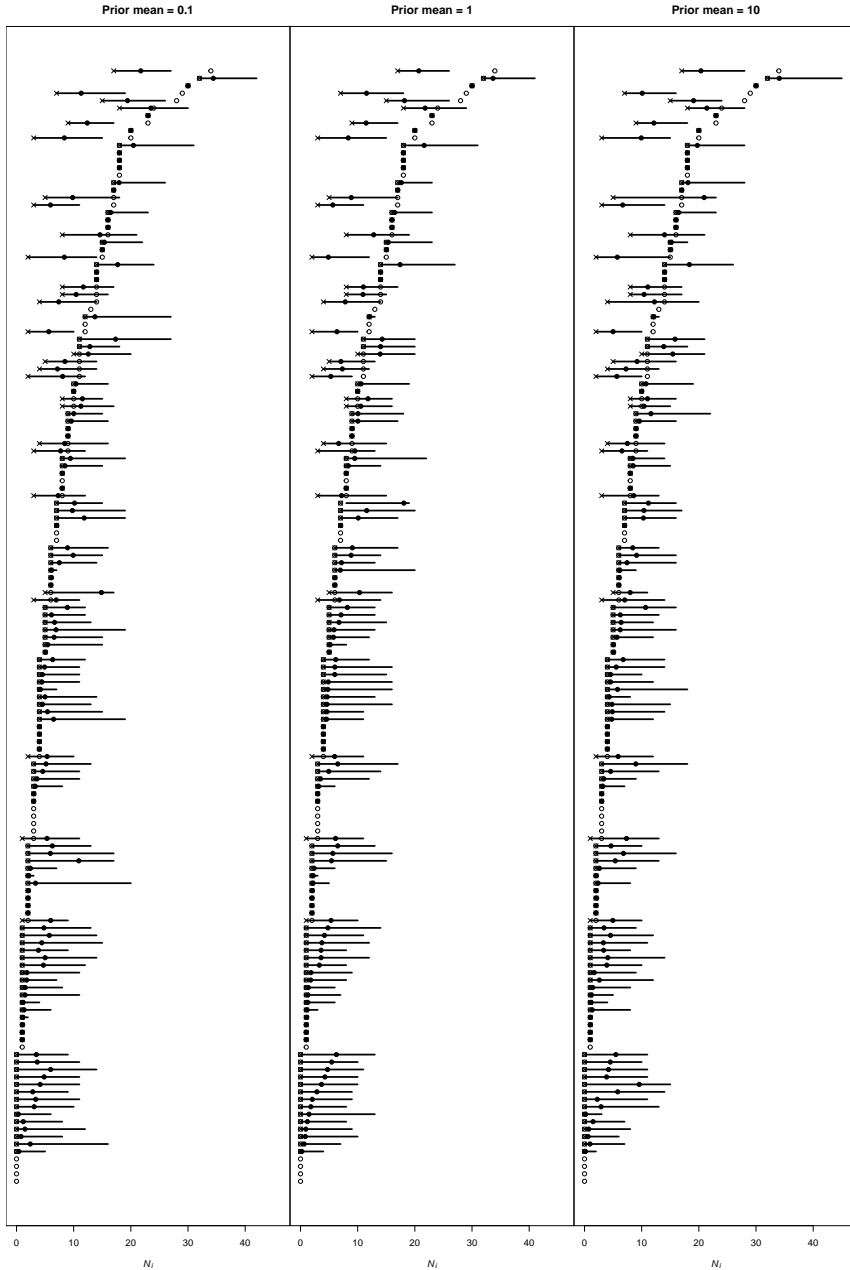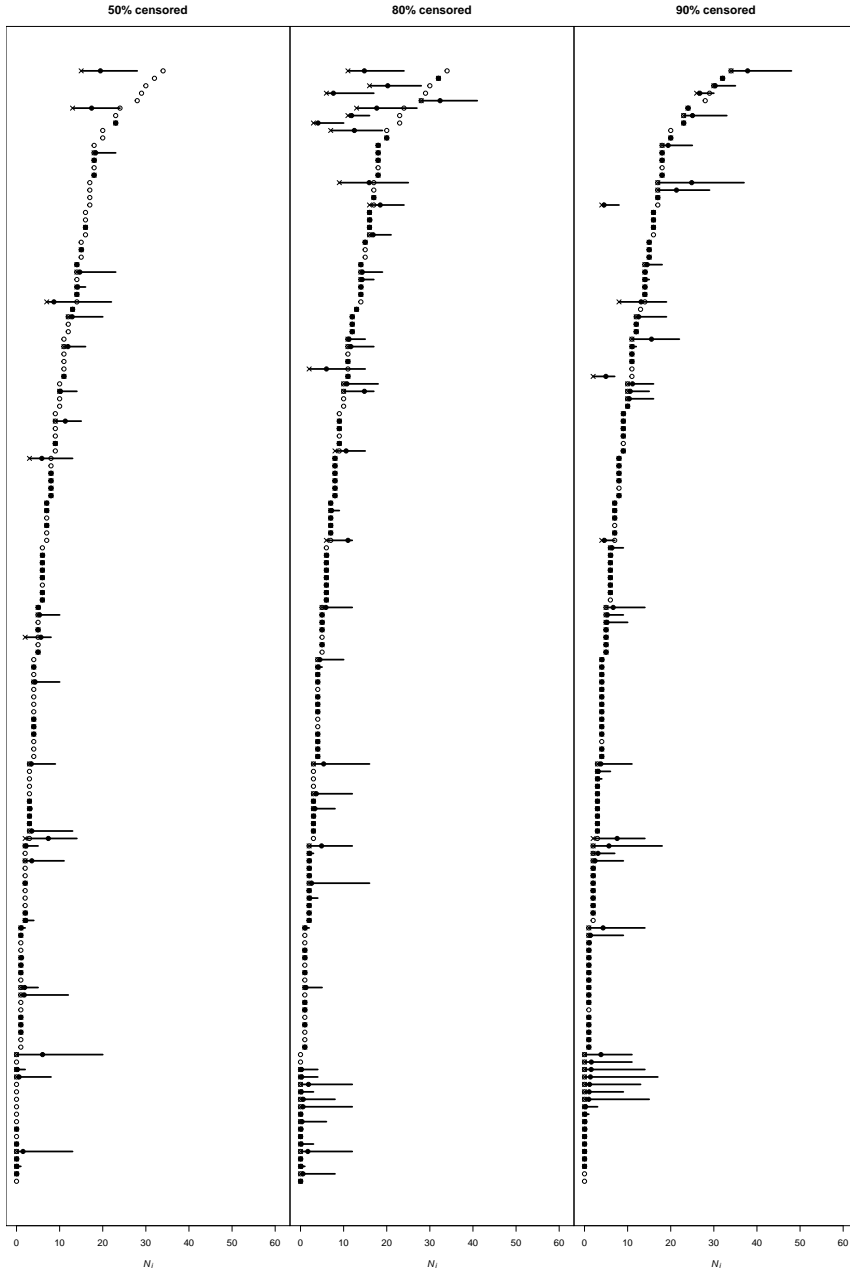
Figure S1: The number of gap times N_i (circle) and, if applicable, their posterior means (dot) and 95% posterior credible intervals (lines) for each individual from our model fitted on the simulated data with 90% censoring and different prior means for λ. For censored individuals, the number of observed gap times n_i is marked by '×'.

10

Figure S2: The number of gap times N_i (circle) and, if applicable, their posterior means (dot) and 95% posterior credible intervals (lines) for each individual from our misspecified model fitted on the data simulated from a Gompertz distribution. For censored individuals, the number of observed gap times n_i is marked by '×'.

11
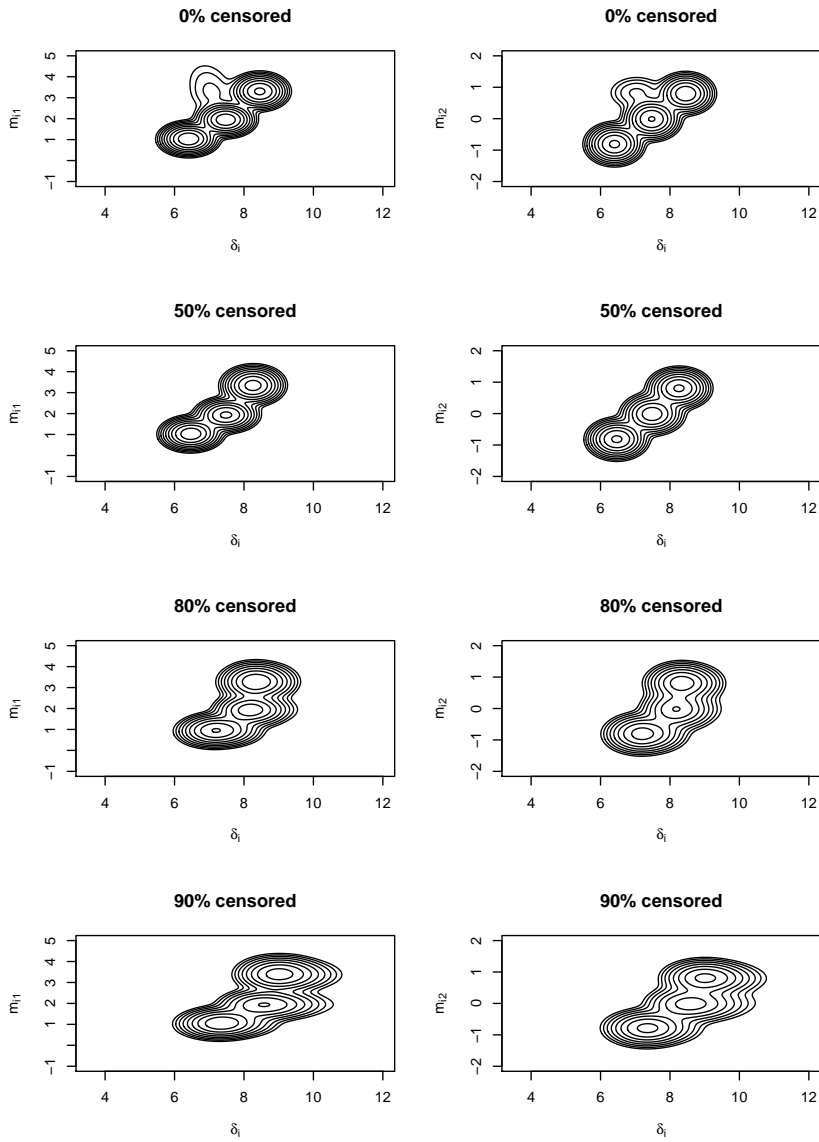
Figure S3: Contour plots of the log of the bivariate posterior predictive densities of (m_{i1}, δ_i) (left) and (m_{i2}, δ_i) (right) for a hypothetical new individual from the data simulated from a Gompertz distribution.
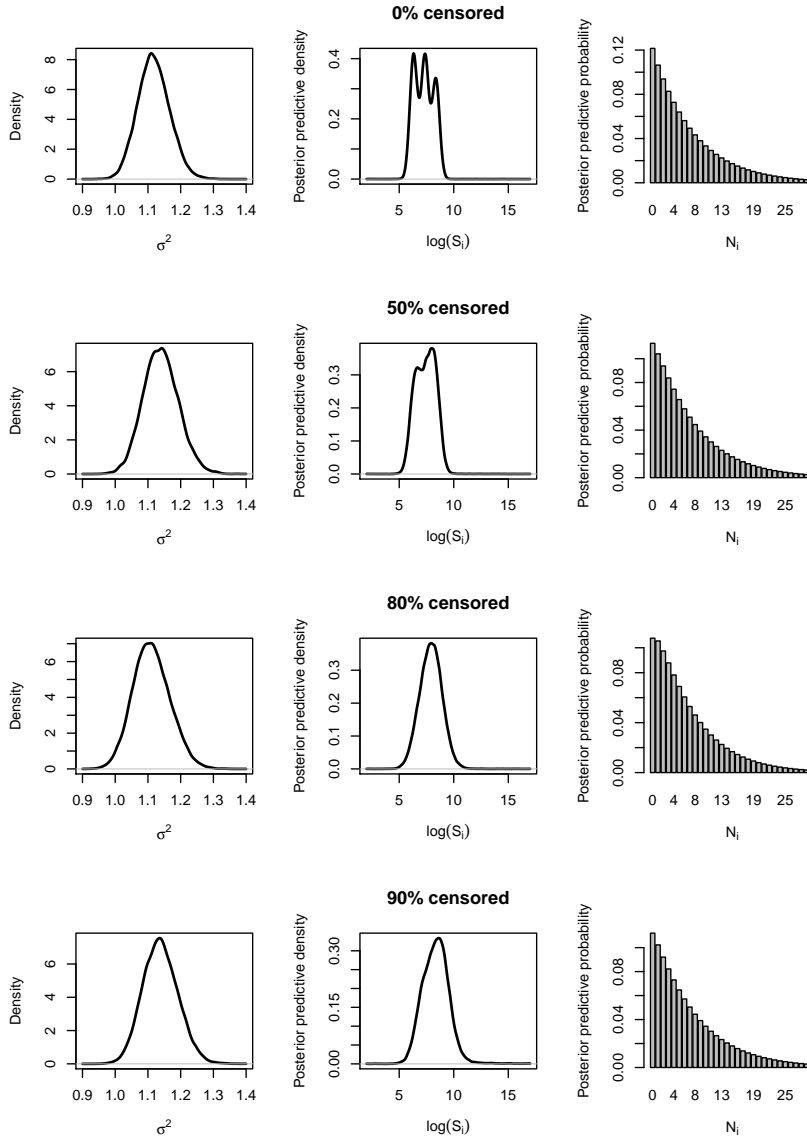
Figure S4: Posterior density for σ^2, and posterior predictive density for $\log(S_i)$ and posterior predictive probability mass function for N_i for a hypothetical new patient with covariates equal to their sample medians from our misspecified model fitted on the data simulated from a Gompertz distribution.

13
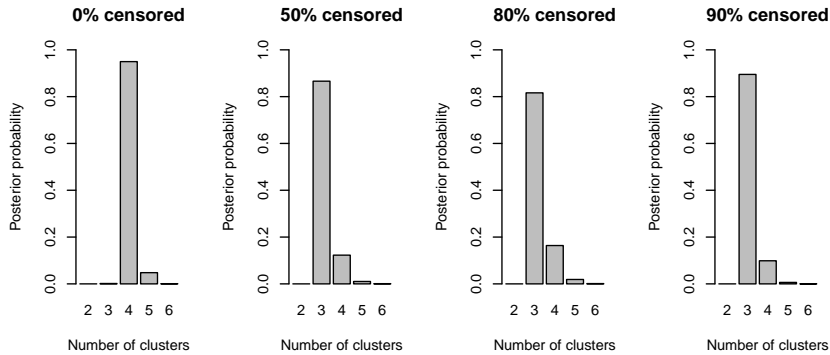
Figure S5: Posterior distribution of the number of clusters from our misspecified model fitted on the data simulated from a Gompertz distribution.
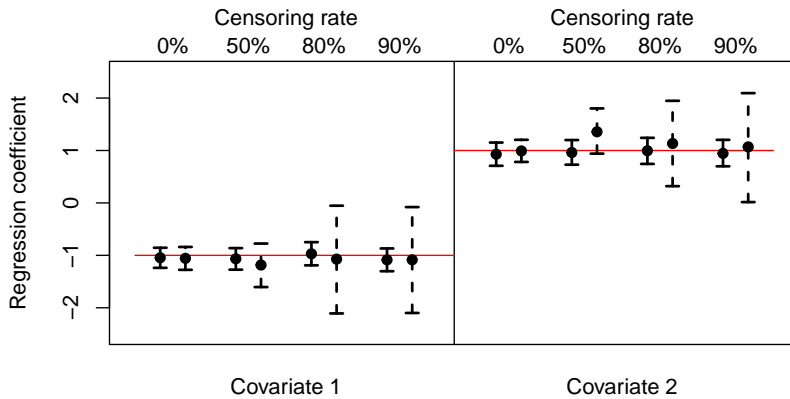
Figure S6: Posterior means (dot) and 95% marginal posterior credible intervals (lines) of the regression coefficients from our misspecified model fitted on the data simulated from a Gompertz distribution. The solid lines represent credible intervals for the regression coefficients $\boldsymbol{\beta}$ in (3) for the gap times model. The dashed lines correspond with the regression coefficients $\boldsymbol{\gamma}$ in (4) for the survival times. The horizontal line marks the true $\boldsymbol{\beta} = \boldsymbol{\gamma} = (-1, 1)^T$ from which the data were simulated.

Table S1: Bias (root mean squared error) of posterior means from our model fitted on simulated data.

Parameter	β_1	β_2	γ_1	γ_2
0% censored	0.16 (0.38)	-0.13 (0.36)	0.00066 (0.20)	-0.22 (0.45)
50% censored	0.17 (0.38)	-0.13 (0.36)	-0.02 (0.23)	-0.15 (0.46)
80% censored	0.089 (0.25)	-0.12 (0.24)	-0.32 (0.69)	0.088 (0.79)
90% censored	0.071 (0.17)	-0.025 (0.16)	0.18 (1.05)	-0.25 (0.70)

Parameter	m_{11}^*	m_{21}^*	m_{31}^*
0% censored	0.20 (0.21)	0.047 (0.073)	-0.29 (0.31)
50% censored	0.33 (0.33)	0.12 (0.14)	-0.25 (0.29)
80% censored	0.44 (0.44)	0.23 (0.25)	-0.21 (0.24)
90% censored	0.45 (0.46)	0.18 (0.26)	-0.26 (0.29)

Parameter	m_{12}^*	m_{22}^*	m_{32}^*
0% censored	0.18 (0.19)	0.036 (0.071)	-0.22 (0.22)
50% censored	0.27 (0.28)	0.077 (0.11)	-0.25 (0.26)
80% censored	0.33 (0.33)	0.11 (0.13)	-0.26 (0.26)
90% censored	0.35 (0.35)	0.11 (0.13)	-0.28 (0.28)

Parameter	δ_1^*	δ_2^*	δ_3^*
0% censored	0.37 (0.51)	0.14 (0.26)	-0.17 (0.24)
50% censored	0.84 (0.93)	0.57 (0.67)	0.18 (0.38)
80% censored	1.65 (1.74)	1.59 (1.67)	1.22 (1.30)
90% censored	2.92 (3.11)	2.59 (2.64)	2.97 (3.17)

S4 Application to atrial fibrillation data

S4.1 Background

In addition to the colorectal cancer data considered in Section 4, we apply our model to data on atrial fibrillation (AF) described in Schroder et al. (2019b) AF is the most common serious cardiac arrhythmia with more than 33 million cases worldwide, increasing rapidly with five million new cases per year (Chung et al., 2020). It is characterized by an irregular and often high heart rate where the heart's upper chambers beat out of sync with its lower chambers. AF causes substantial morbidity and mortality, for instance due to heart failure and stroke. It places a high burden on health care systems, constituting 2.4% of the United Kingdom's National Health Service budget in 2000 (Thrall et al., 2006).

AF is often a chronic condition that requires repeated treatment. The goal of these treatments is to reduce the rate of AF episodes, as an increased number of episodes is associated with complications such as stroke (Munger et al., 2014). Thus, there is dependence between recurrence and survival, which our model is able to capture. Additionally, more frequent AF events are associated with an increase in the rate of episodes going forward (Wijffels et al., 1995). This points to temporal dependence in the AF recurrence process, as captured in our model by (3).

A variety of treatments exist. These include prophylactic anti-arrhythmic medication and cardioversion (Schroder et al., 2019b). Anti-arrhythmic medication aims to reduce the rate and duration of AF episodes. Cardioversion aims to restore the heart rhythm when it is abnormal, that is while someone is experiencing an AF episode. Cardioversion is either electrical, using direct currents, or pharmacologic. Electrical cardioversion takes place in a hospital. AF diagnosis usually requires an electrocardiogram (ECG).

The condition of AF can be categorized into three subtypes: paroxysmal, persistent and permanent (January et al., 2014). Episodes of paroxysmal AF terminate spontaneously without treatment. In contrast, persistent AF is when the episode only ends due to an intervention. Lastly, AF is permanent when the patient and clinician decide to no longer attempt to restore the heart rhythm. Additionally, AF episodes are either symptomatic or asymptomatic. Symptoms of AF include palpitations and chest pain.

As for many other chronic diseases, clinical interest lies in both the final outcome (death or survival time) and the dynamics of the process itself, since it determines the subsequent quality of the patient's life (Thrall et al., 2006). From an economic and healthcare planning perspective, there is great interest in reducing rehospitalization for AF. In fact, a better understanding of both death and non-fatal clinical events could lead to improved prognosis and assessment of the impact and costs of AF by health providers. It is, therefore, of paramount importance to develop a comprehensive model for disease management, mortality and associated clinical event histories, which also accounts for the significant interindividual variability in disease course as it is typical of chronic diseases and biological events, and can infer the number of rehospitalizations as it closely relates to economic cost.

Table S2: Frequency table of the number of observed gap times n_i in the AF data.

n_i	0	1	2	3	4	5	6	7	8	9	10	11	12	13	14	15	16
Frequency	29	11	9	9	3	3	9	4	2	0	2	1	0	1	0	0	1

S4.2   Data description and analysis

The data (Schroder et al., 2019a) consist of hospitalizations from January 1, 2008 to March 1, 2014 at the Department of Cardiology at University Hospital Copenhagen, Hvidovre, Denmark (Schroder et al., 2019b). The primary reason of all hospitalizations is symptomatic AF. Some include cardioversion treatment. AF is confirmed by ECG. We consider $L = 84$ patients that experience at least one hospitalization due to non-permanent AF. This first hospitalization represents the origin of a patient's recurrence process such that $T_{i0} = 0$ for all i. Using an event time as origin is standard practice in models for gap times (Cook and Lawless, 2007), though a different origin, if available, could be chosen to also include individuals who experience no events. Consequently, n_i represents the number of observed gap times between subsequent hospitalizations due to non-permanent AF. Patients experience between zero and 16 rehospitalizations each and $\sum_{i=1}^{L} n_i = 241$ in aggregate. Table S2 shows how they are distributed across patients. Gap times are defined as the difference between successive hospitalizations and, as such, capture both the length of stay in the hospital and the time between discharge and the next hospitalization.

The main clinical outcome of interest is deterioration to permanent AF or death. We therefore define the survival time S_i as the time to permanent AF or death. The survival times of 68 out of the 84 recurrence processes are censored due to the follow-up ending on March 1, 2014, resulting in unobserved total number of gap times N_i.

Patient characteristics are determined at the first hospitalization. They are 1) age; and the binary variables 2) gender; whether 3) AF is paroxysmal or persistent; and whether the patient has 4) hypertension; 5) heart disease; or 6) is on anti-arrhythmic medication. Here, heart disease includes heart failure, heart valve disease and ischemic heart disease. These variables form the subject-specific 6-dimensional covariate vector $\boldsymbol{x}_i$, with $q = 6$. Being older or female, hypertension, and heart disease are known to be associated with more severe AF (January et al., 2014). Anti-arrhythmic medication aims to prevent and ameliorate the reoccurrence of AF. We standardize the age in $\boldsymbol{x}_i$. Table S3, and Figures S7 and S8 summarize the patient characteristics, and the gap and survival times.

We use the same priors, from Section S2, and set-up of the Gibbs sampler as the simulation study in Section 3.

S4.3   Posterior inference

The posterior inference is summarized in Figures S9 through S13 analogously to the colorectal cancer application in Section 4.

Figure S9 summarizes the posterior distribution of the total number of gap times N_i for each patient. The posterior means for the censored N_i are generally in line with the observed

Table S3: Summary statistics of the AF data and the posterior from our model. The averages and standard deviations of posterior means are taken across patients and recurrent events. S_i is recorded in days and Y_{ij} in log days.

Number of patients	841
Proportion censored	81%
Average uncensored N_i	1.75 (2.15)
Average posterior mean of N_i (SD)	3.99 (3.72)
Average uncensored Y_{ij} (SD)	4.17 (1.61)
Average posterior mean of Y_{ij} (SD)	4.72 (1.26)
Average uncensored $\log(S_i)$ (SD)	5.72 (1.25)
Average posterior mean of $\log(S_i)$ (SD)	11.6 (3.27)
Average age (SD)	58.2 (12.2)
Proportion female	32%
Proportion with paroxysmal AF	15%
Proportion with hypertension	46%
Proportion with heart disease	20%
Proportion on anti-arrhythmic medication	12 %
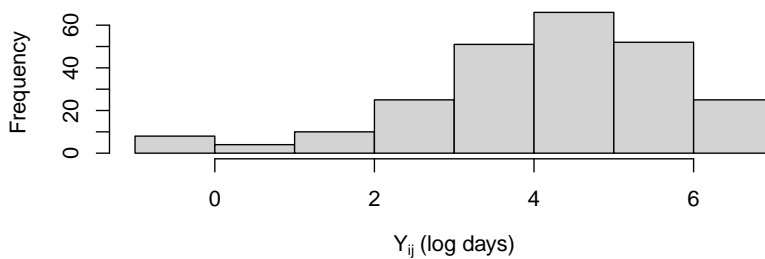
Figure S7: Histogram of the 241 observed log gap times Y_{ij} in the AF data.

18
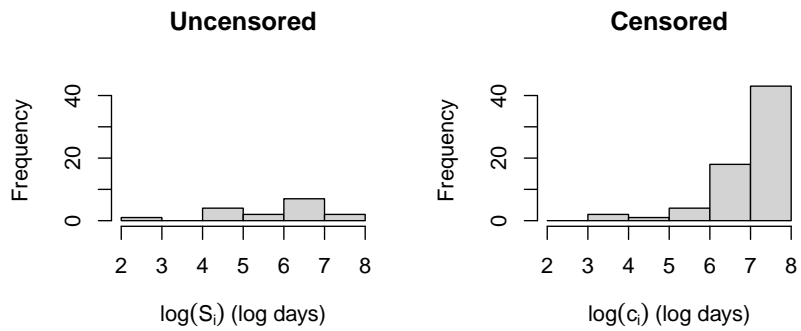
Figure S8: Histograms of the log of the 16 observed survival times S_i (left) and the 68 censoring times (right) in the AF data. If the survival time S_i is observed, then $c_i = S_i$.
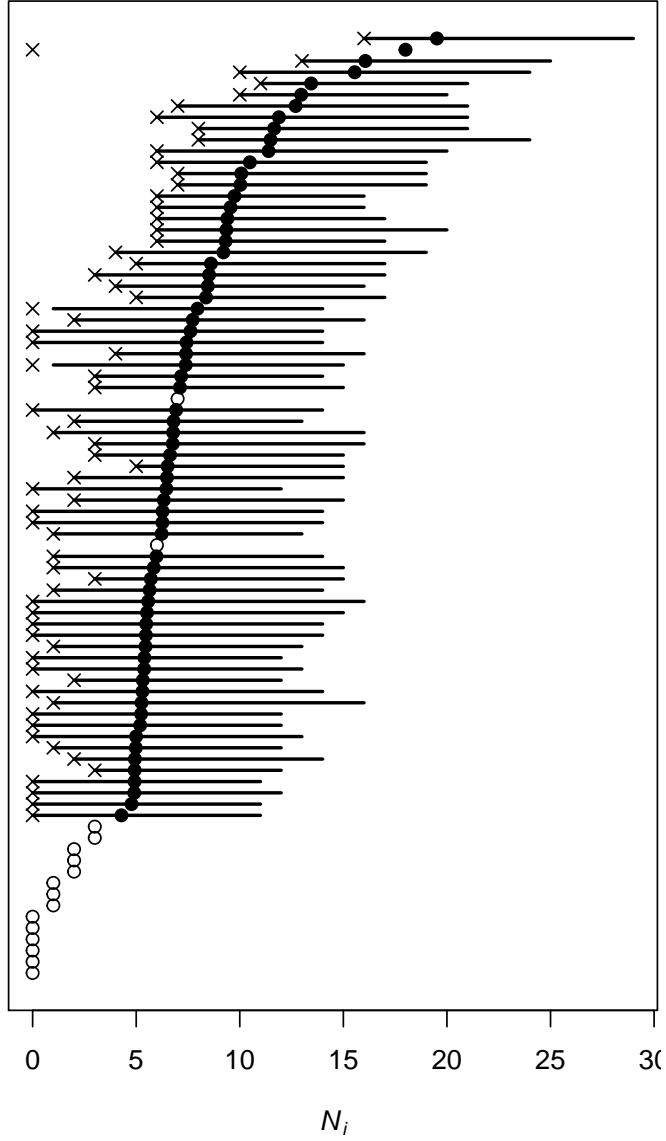
Figure S9: The number of gap times N_i (circle) if observed and otherwise their posterior means (dot) and 95% posterior credible intervals (lines) for each patient from our model fitted on the AF data. For censored patients, the number of observed gap times n_i is marked by '×'.
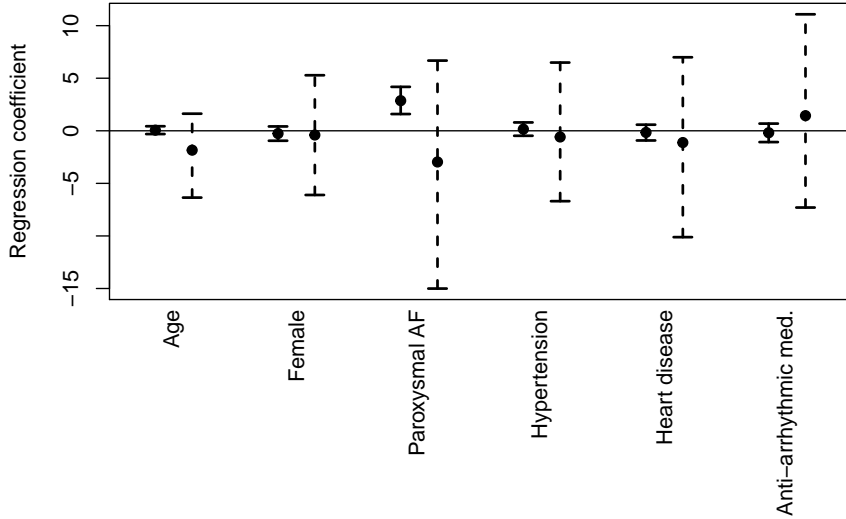
Figure S10: Posterior means (dot) and 95% marginal posterior credible intervals (lines) of the regression coefficients from our model fitted on the AF data. The solid lines represent credible intervals for the regression coefficients $\boldsymbol{\beta}$ in (3) for the gap times model. The dashed lines correspond with the regression coefficients $\boldsymbol{\gamma}$ in (4) for the survival times.

N_i. The unobserved N_i are sometimes inferred to be larger than the largest observed N_i. After all, the largest observed N_i equals seven while the number of observed gap times n_i is 16 for one patient. This is expected since patients with longer survival times S_i are both more likely to have a higher number of gap times N_i and to be censored due to end of study.

Figure S10 shows no evident effect of any of the covariates as the corresponding 95% credible intervals include 0, except for the interval for the effect of paroxysmal AF on gap times which excludes zero. This is in line with the analysis of these data described in Schroder et al. (2019b) The relatively small sample size of $L = 84$ might be the reason that we do not find strong effects, even though most of these covariates are risk factors for AF.

Figure S11 shows that the posterior marginals of (m_{i1}, δ_i) and (m_{i2}, δ_i) are unimodal. The cluster allocation that minimizes the posterior expectation of Binder's(Binder, 1978) loss function confirms this with all subjects clustered together. Finally, Figure S13 also has the posterior mode at one cluster.

S4.4   Comparison with other models

We consider that same model comparisons for the AF data as we did for the colorectal cancer data in Section 5. The results are presented in Figures S14 through S16, and Tables S4 and S5.

When fitting the Cox proportional hazard model, we include a patient's log mean gap
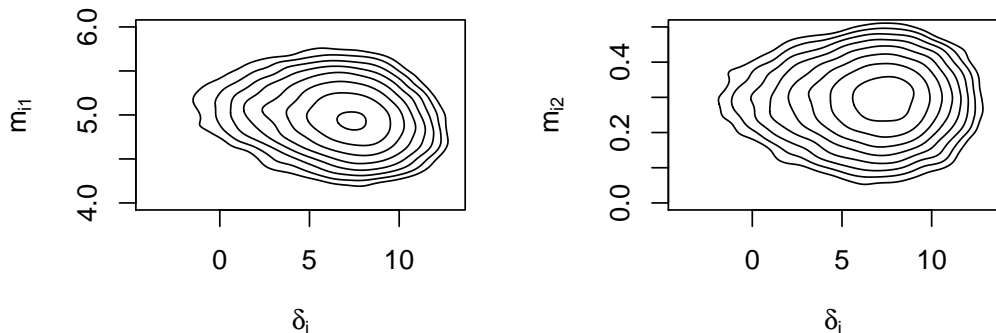
Figure S11: Contour plots of the log of the bivariate posterior predictive densities of (m_{i1}, δ_i) (left) and (m_{i2}, δ_i) (right) for a hypothetical new patient from the AF data.
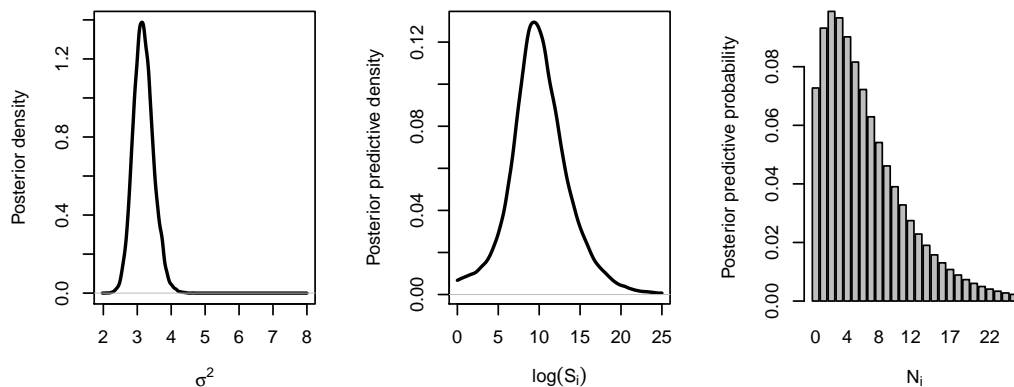

Figure S12: Posterior density for σ^2, and posterior predictive density for $\log(S_i)$ and posterior predictive probability mass function for N_i for a hypothetical new patient with binary covariates equal to their sample mode and with age equal to the sample median from our model fitted on the AF data.
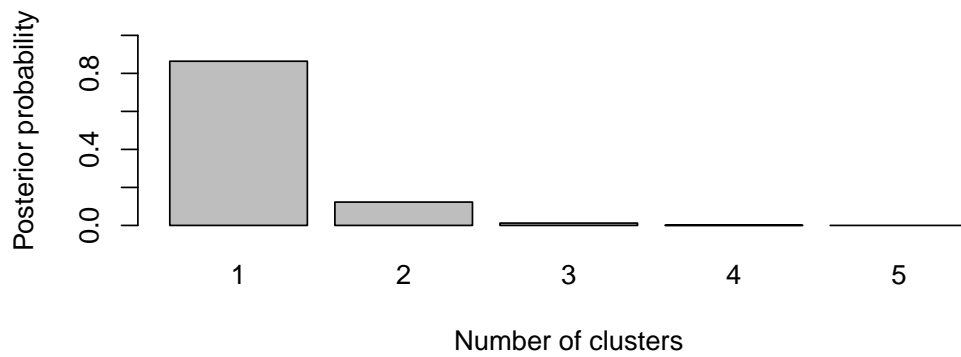
Figure S13: Posterior distribution of the number of clusters from our model fitted on the AF data.

Table S4: Regression coefficients from the Cox proportional hazards model fitted on the AF data.

Covariate	Hazard ratio	95% CI
Age	2.06	(0.95, 4.47)
Female	1.33	(0.30, 5.92)
Paroxysmal AF	3.55	(0.36, 35.4)
Hypertension	1.02	(0.22, 4.83)
Heart disease	1.12	(0.19, 6.52)
Antiarrhythmic medication	0.50	(0.06, 4.55)
Log mean gap time	1.22	(0.73, 2.05)

time in the covariate vector z_i in addition to the six covariates included in x_i described in Section S4.2. As a result, the 29 individuals with no observed gap times are excluded. Table S4 shows the covariate effects on survival from the Cox proportional hazards model. They agree with the inference for γ from our model in Figure S10 in that they do not exhibit a significant effect.

To fit the joint frailty model (Rondeau et al., 2007) to the AF data, we drop hypertension from x_i due to convergence issues when using all covariates. The comparison of the joint frailty model results in Table S5 with our results in Figure S10 shows that both models obtain similar results and do not detect an association for most of the covariates while agreeing that paroxysmal AF reduces the rehospitalization rate. The models disagree on the effect of age on rehospitalization and survival, where the joint frailty model finds a statistically significant effect. Finally, the estimate of ρ is 0.007 with a standard error of 0.001. This suggests heterogeneity between patients that is not explained by the covariates even though our model detected only a single cluster.

The Bayesian semi-parametric model from Paulon et al. (2018) yields conclusions that are largely consistent with those from our model. In particular, the posterior distributions on the coefficients in Figure S14 closely mimic our results in Figure S10. Also, the posterior on ψ in (5) concentrates between 1.5 and 3.5 per Figure S15. This parameter captures the strength of the relationship between gap and survival times. Thus, the time between hospitalizations and survival have a positive association. This is consistent with the dependence implied by the truncation $T_{iN_i} \le S_i$ in our model. Lastly, the posterior on the number of clusters for this model and our model vary slightly, with the mode at one clusters for our model in Figure S13 while Figure S16 has the mode at four. This is not surprising as discussed in Section 5.3.

References

Aalen, O. O. and Husebye, E. (1991) Statistical analysis of repeated events forming renewal processes. *Statistics in Medicine*, **10**, 1227–1240.

Asmussen, S., Goffard, P.-O. and Laub, P. J. (2019) Orthonormal polynomial expansions and

Table S5: Regression coefficients from the joint frailty model fitted on the AF data.

Rehospitalization

Covariate	Hazard ratio	p-value
Age	1.01	0.04
Female	0.90	0.46
Paroxysmal AF	0.59	0.03
Heart disease	0.93	0.64
Antiarrhythmic medication	0.73	0.07

Mortality

Covariate	Hazard ratio	p-value
Age	1.10	0.04
Female	4.22	0.10
Paroxysmal AF	1.68	0.59
Heart disease	2.03	0.37
Antiarrhythmic medication	1.81	0.52
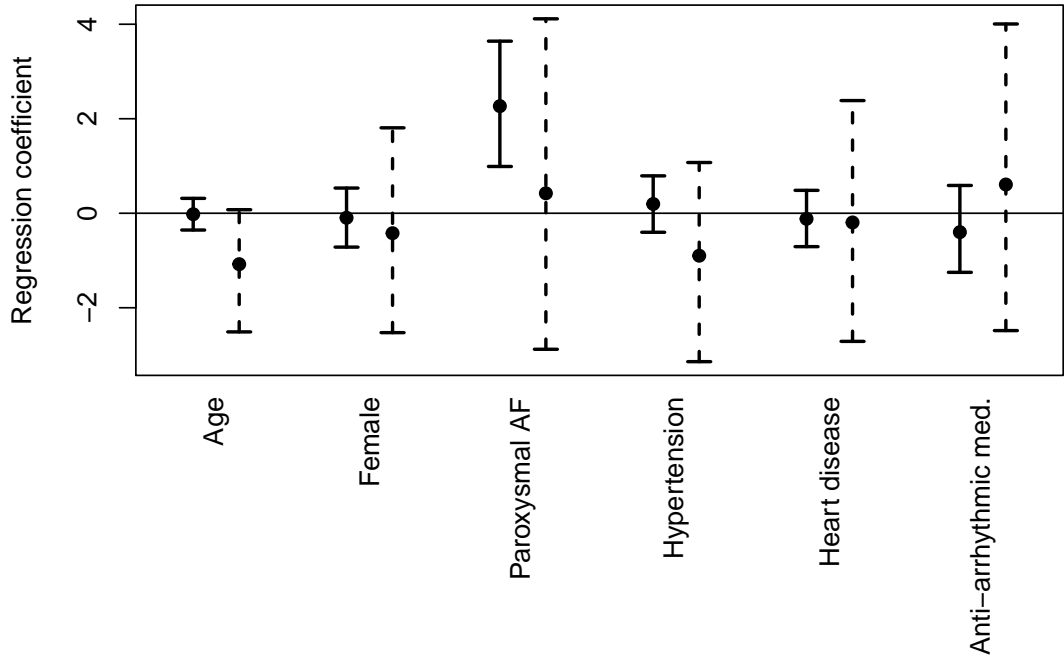
Figure S14: Posterior means (dot) and 95% marginal posterior credible intervals (lines) of the regression coefficients from the model in Paulon et al. (2018) fitted on the AF data. The solid lines represent credible intervals for the regression coefficients $\boldsymbol{\beta}$ in the gap times model. The dashed lines correspond to the regression coefficients $\boldsymbol{\gamma}$ in (5) for the survival times.
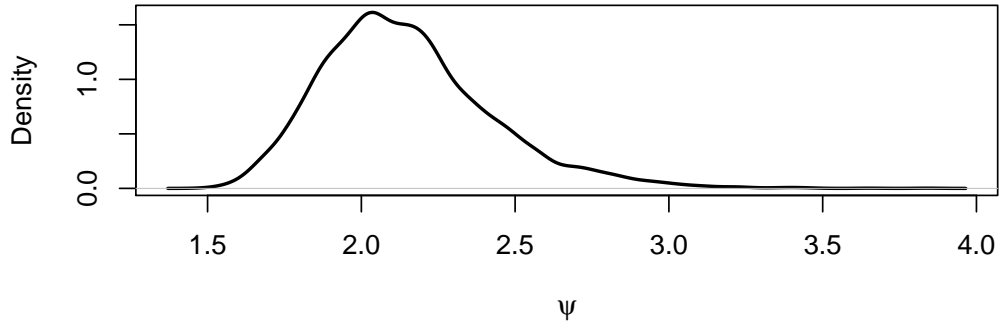
Figure S15: Posterior density for ψ in (5) from the model in Paulon et al. (2018) fitted on the AF data.
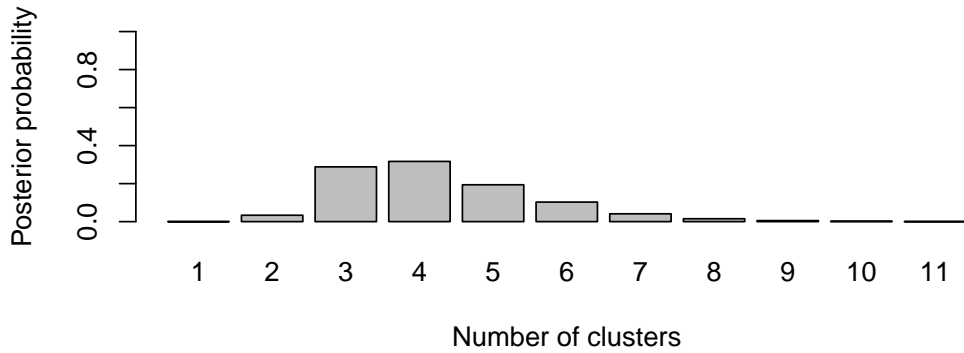
Figure S16: Posterior distribution of the number of clusters from the model from Paulon et al. (2018) fitted on the AF data.

lognormal sum densities. In *Risk and Stochastics*, 127–150. World Scientific.

Asmussen, S., Jensen, J. L. and Rojas-Nandayapa, L. (2016) Exponential family techniques for the lognormal left tail. *Scandinavian Journal of Statistics*, **43**, 774–787.

Binder, D. A. (1978) Bayesian cluster analysis. *Biometrika*, **65**, 31–38.

Botev, Z. I., Salomone, R. and Mackinlay, D. (2019) Fast and accurate computation of the distribution of sums of dependent log-normals. *Annals of Operations Research*, **280**, 19–46.

Chung, M. K., Eckhardt, L. L., Chen, L. Y., Ahmed, H. M., Gopinathannair, R., Joglar, J. A., Noseworthy, P. A., Pack, Q. R., Sanders, P. and and, K. M. T. (2020) Lifestyle and risk factor modification for reduction of atrial fibrillation: A scientific statement from the american heart association. *Circulation*, **141**.

Cook, R. J. and Lawless, J. F. (2007) *The statistical analysis of recurrent events*. Springer, New York.

Escobar, M. D. and West, M. (1995) Bayesian density estimation and inference using mixtures. *Journal of the American Statistical Association*, **90**, 577–588.

Fenton, L. (1960) The sum of log-normal probability distributions in scatter transmission systems. *IEEE Transactions on Communications*, **8**, 57–67.

Green, P. J. (1995) Reversible jump Markov chain Monte Carlo computation and Bayesian model determination. *Biometrika*, **82**, 711–732.

Halliwell, L. J. (2015) The lognormal random multivariate. *Casualty Actuarial Society E-Forum*, **Spring 2015**, 1–5.

January, C. T., Wann, L. S., Alpert, J. S., Calkins, H., Cigarroa, J. E., Cleveland, J. C., Conti, J. B., Ellinor, P. T., Ezekowitz, M. D., Field, M. E., Murray, K. T., Sacco, R. L., Stevenson, W. G., Tchou, P. J., Tracy, C. M. and Yancy, C. W. (2014) 2014 AHA/ACC/HRS guideline for the management of patients with atrial fibrillation. *Circulation*, **130**.

Munger, T. M., Wu, L.-Q. and Shen, W. K. (2014) Atrial fibrillation. *Journal of Biomedical Research*, **28**, 1–17.

Neal, R. M. (2000) Markov chain sampling methods for Dirichlet process mixture models. *Journal of Computational and Graphical Statistics*, **9**, 249–265.

Paulon, G., De Iorio, M., Guglielmi, A. and Ieva, F. (2018) Joint modeling of recurrent events and survival: A Bayesian non-parametric approach. *Biostatistics*. Kxy026.

Rondeau, V., Mathoulin-Pelissier, S., Jacqmin-Gadda, H., Brouste, V. and Soubeyran, P. (2007) Joint frailty models for recurring events and death using maximum penalized likelihood estimation: Application on cancer events. *Biostatistics*, **8**, 708–721.

Schroder, J., Bouaziz, O., Agner, B. R., Martinussen, T., Madsen, P. L., Li, D. and Dixen, U. (2019a) Full anonymized dataset used for statistical analysis. *figshare, doi:10.1371/journal.pone.0217983.s001.*

— (2019b) Recurrent event survival analysis predicts future risk of hospitalization in patients with paroxysmal and persistent atrial fibrillation. *PLOS ONE*, **14**, e0217983.

Tallarita, M., De Iorio, M., Guglielmi, A. and Malone-Lee, J. (2020) Bayesian autoregressive frailty models for inference in recurrent events. *The International Journal of Biostatistics*, **16**, 1–18.

Thrall, G., Lane, D., Carroll, D. and Lip, G. Y. (2006) Quality of life in patients with atrial fibrillation: A systematic review. *The American Journal of Medicine*, **119**, 448.e1–448.e19.

Waagepetersen, R. and Sorensen, D. (2001) A tutorial on reversible jump MCMC with a view toward applications in QTL-mapping. *International Statistical Review*, **69**, 49–61.

Wijffels, M. C., Kirchhof, C. J., Dorland, R. and Allessie, M. A. (1995) Atrial fibrillation begets atrial fibrillation. *Circulation*, **92**, 1954–1968.

Table S6: Regression coefficients from the Cox proportional hazards model fitted on the colorectal cancer data.

Covariate	Hazard ratio	95% CI
Chemotherapy	1.56	(0.96, 2.54)
Female	0.55	(0.33, 0.93)
Stage C	2.91	(1.40, 6.04)
Stage D	11.5	(5.58, 23.5)
Log mean gap time	0.88	(0.74, 1.04)

Table S7: Regression coefficients from the joint frailty model fitted on the colorectal cancer data.

Rehospitalization

Covariate	Hazard ratio	p-value
Chemotherapy	0.86	0.30
Female	0.60	0.00
Stage C	1.53	0.01
Stage D	4.27	0.00

Mortality

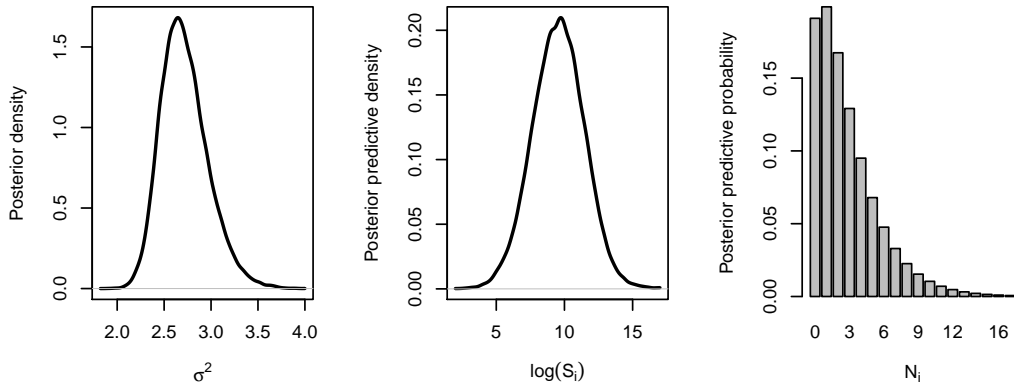| Covariate	Hazard ratio	p-value
Chemotherapy	2.70	0.00
Female	0.76	0.24
Stage C	4.91	0.00
Stage D	52.8	0.00

Figure S17: Posterior density for σ^2, and posterior predictive density for $\log(S_i)$ and posterior predictive probability mass function for N_i for a hypothetical new patient with covariates equal to their sample mode from our model fitted on the colorectal cancer data.
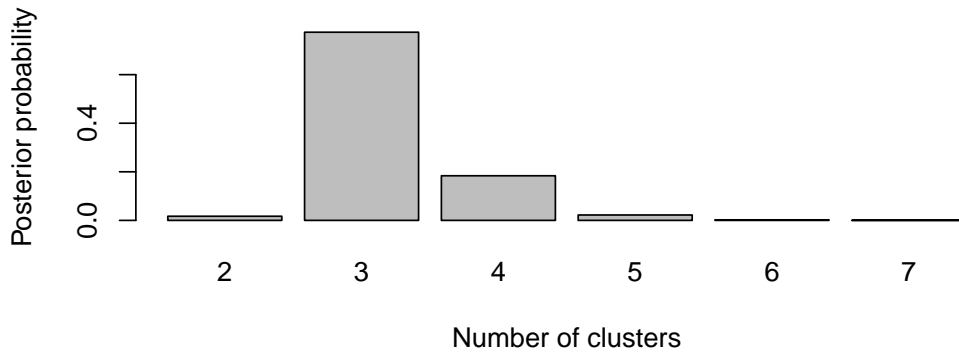

Figure S18: Posterior distribution of the number of clusters from our model fitted on the colorectal cancer data.
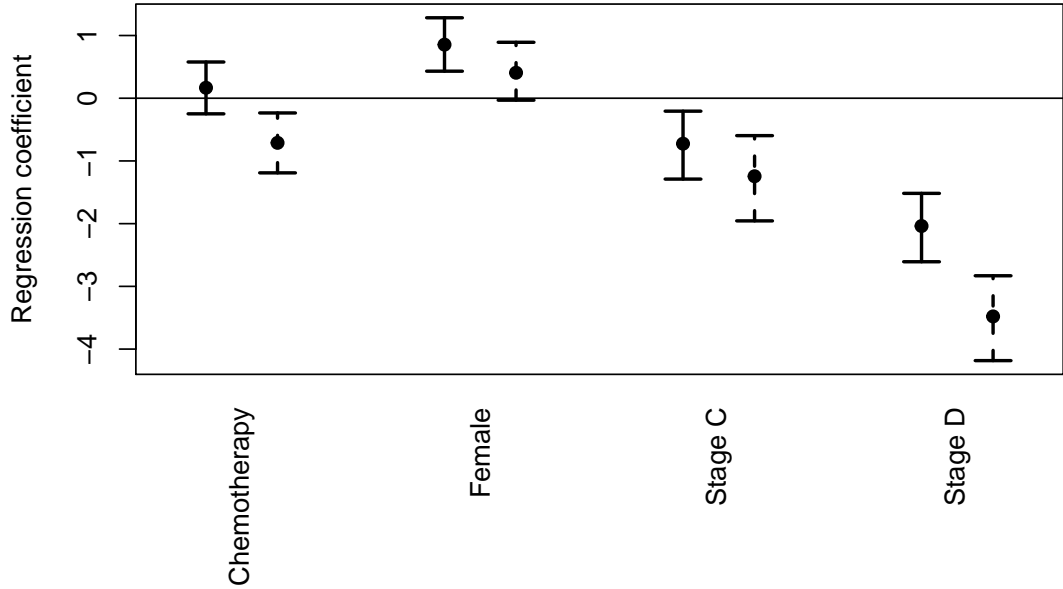
Figure S19: Posterior means (dot) and 95% marginal posterior credible intervals (lines) of the regression coefficients from the model in Paulon et al. (2018) fitted on the colorectal cancer data. The solid lines represent credible intervals for the regression coefficients $\boldsymbol{\beta}$ in the gap times model. The dashed lines correspond to the regression coefficients $\boldsymbol{\gamma}$ in (5) for the survival times.
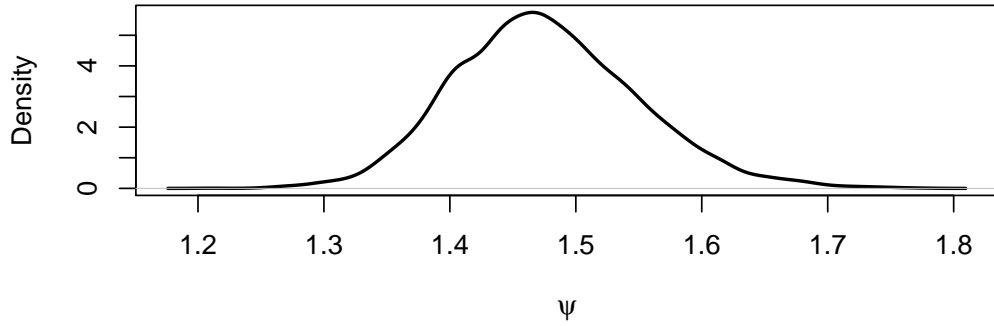
Figure S20: Posterior density for ψ in (5) from the model in Paulon et al. (2018) fitted on the colorectal cancer data.
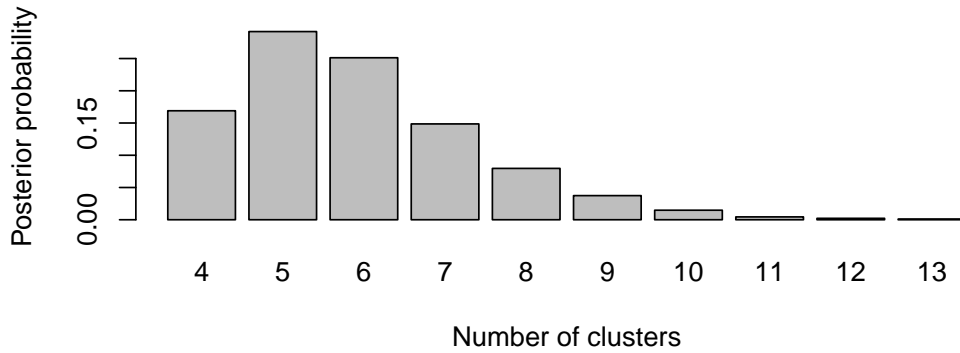

Figure S21: Posterior distribution of the number of clusters from the model from Paulon et al. (2018) fitted on the colorectal cancer data.